Received: 16 October 2023 | Accepted: 6 December 2023

DOI: 10.1002/ppj2.20092

The Plant Phenome Journal OPEN ACCESS

ORIGINAL ARTICLE

# Genetics of canopy architecture dynamics in photoperiod-sensitive and photoperiod-insensitive sorghum

**Juan S. Panelo**[1] | **Yin Bao**[2] | **Lie Tang**[2] | **Patrick S. Schnable**[1] | **Maria G. Salas-Fernandez**[1]

[1]Department of Agronomy, Iowa State University, Ames, Iowa, USA

[2]Department of Agricultural and Biosystems Engineering, Iowa State University, Ames, Iowa, USA

**Correspondence**
Maria G. Salas-Fernandez, Department of Agronomy, Iowa State University, Ames, IA, USA. Email: mgsalas@iastate.edu

Assigned to Associate Editor Michael Gore.

**Present address**
Yin Bao, Department of Mechanical Engineering, University of Delaware, Newark, Delaware, USA.

**Funding information**
National Institute of Food and Agriculture, Grant/Award Numbers: 2012-67009-19713, IOW04314; Plant Sciences Institute at Iowa State University

## Abstract

Canopy architecture traits are associated with productivity in sorghum [*Sorghum bicolor* (L.) Moench], and they are commonly measured at the time of flowering or harvest. Little is known about the dynamics of canopy architecture traits through the growing season. Utilizing the ground-based high-throughput phenotyping system Phenobot 1.0, we collected stereo images of a photoperiod-sensitive and a photoperiod-insensitive population over time to generate three-dimensional (3D) representations of the canopy. Four descriptors were automatically extracted from the 3D point clouds: plot-based plant height (PBPH), plot-based plant width (PBPW), plant surface area (PSA), and convex hull volume (CHV). Additionally, genotypic growth rates were estimated for each canopy descriptor. Genome-wide association analysis was performed on individual timepoints and the growth rates in both populations. We detected genotypic variation for each of the four canopy descriptors and their growth rates and discovered novel genomic regions associated with growth rates on chromosomes 1 (PBPH, CHV), 3 (PBPH), 4 (PBPH, PBPW), 5 (PBPH), 8 (PSA), and 9 (PBPW). These results provide new knowledge about the genetic control of canopy architecture, highlighting genomic regions that can be targeted in plant breeding programs.

**Abbreviations:** AABB, axis-aligned bounding box; AEARF, Agricultural Engineering and Agronomy Research Farm; BLUP, best linear unbiased predictor; CHV, convex hull volume; GBS, genotyping by sequencing; GWAS, genome-wide association study; HTPS, high-throughput phenotyping systems; MAF, minor allele frequency; ME, malic enzyme; MCMC, Monte Carlo Markov chain; MTA, marker-trait associations; PBPH, plot-based plant height; PBPW, plot-based plant width; PSP, Photoperiod-Sensitive Panel; PVE, phenotypic variance explained; QTL, quantitative trait loci; QTN, quantitative trait nucleotide; SAP, Sorghum Association Panel; SNP, single nucleotide polymorphism; tGBS, tunable genotyping by sequencing; UAV, unmanned aerial vehicle; WAP, weeks after planting; 3D, three-dimensional.

## 1 | INTRODUCTION

Canopy architecture has been proposed as a relevant target for crop modeling and plant breeding, given its contribution to crop photosynthesis and ultimately yield (Long et al., 2006; Ort et al., 2015; Song et al., 2013). Canopy architecture is a complex trait that describes how different plant organs such as leaves, stems, tillers, and inflorescences are arranged in three-dimensional (3D) space (Teh et al., 2000). Plant height, leaf angle, and leaf area are commonly utilized to study canopy architecture because these traits are correlated with light interception, stem elongation, and photosynthetic activity (Jaikumar et al., 2021; F. Liu et al., 2021; Mocoeur et al., 2015; Perez et al., 2019; Truong et al., 2015).

Plant height is one of the most extensively studied characteristics of sorghum, and its manipulation has been facilitated by the major effects of the main four dwarfing genes (Quinby & Karper, 1953). In photoperiod-sensitive (PS) sorghums, plant height can reach over 4 m (Brenton et al., 2016; Olson et al., 2012; Rodrigues Castro et al., 2022; Salas-Fernandez & Kemp, 2022; Yu et al., 2016) and is highly correlated with biomass yield (Salas-Fernandez et al., 2009) due to the increased dry matter accumulation in the stems (Olson et al., 2012). The manipulation of leaf angle and leaf area distribution at different canopy layers contributes to improved crop productivity (Mantilla-Perez et al., 2020; Perez et al., 2019; Truong et al., 2015). Smaller (i.e., more upright) leaf angles improve light distribution through the canopy, favoring the photosynthetic activity in the lower layers (Zhi, Massey-Reed, et al., 2022). Improvements in biomass yield have been reported in sorghum as an effect of having upright leaves (Jaikumar et al., 2021; Truong et al., 2015). Leaf area, a proxy for canopy size, is a required component for crop modeling to predict photosynthesis and yield (Weiss et al., 2004). In sorghum, smaller leaf area improved performance in water-limited environments (Borrell et al., 2014), whereas larger leaf area index (leaf area per unit of surface area) has been correlated with higher growth rates in long season genotypes (Goldsworthy, 1970). Lastly, tillering capacity plays an important role in canopy architecture by determining the spatial arrangement of shoots within the row, and thus, canopy volume. In sorghum, tillering capacity is highly correlated with leaf area (George-Jaeggli et al., 2017), and it is associated with higher yields under certain environmental conditions, especially under low planting densities (Kim et al., 2010; Lafarge & Hammer, 2002; Lafarge et al., 2002).

Traits related to canopy architecture have been studied using (i) a genetic approach in which large sets of genotypes are investigated at specific growing stages (Breitzman et al., 2019; Brenton et al., 2016; Mantilla-Perez et al., 2020; Yu et al., 2016; Zhao et al., 2016; Zhi, Tao, et al., 2022) and/or (ii) a physiological approach in which small sets of genotypes are characterized in detail across the entire growing season (Goldsworthy, 1970; Kim et al., 2010; Kouressy et al., 2008; Lafarge et al., 2002; Perrier et al., 2017; Pfeiffer et al., 2019; Truong et al., 2015). Whereas the first approach allows a deeper understanding of physiological processes and their dynamics, the latter provides valuable information about the genetic architecture behind these processes. Even though a combination of both approaches would be beneficial, implementing a physiological approach into genetic studies represents a scalability challenge.

**Core Ideas**

- The range of variation of image-derived canopy architecture descriptors differs between sorghum populations.
- Growth rates can be estimated from canopy descriptors collected over time.
- Natural variation was observed for single-timepoint canopy descriptors and their growth rates.
- Novel genomic regions were associated with single-timepoint canopy descriptors and their growth rates.

The advent of high-throughput phenotyping systems (HTPS) drastically reduced the time required for data collection resulting in an increase in scalability (Bao et al., 2019). The deployment of HTPS facilitated the characterization of canopy architecture and growth rates under controlled conditions in maize (*Zea mays* L.) (Muraya et al., 2017; W. Wang et al., 2023), rice (*Oryza sativa* L.) (Al-Tamimi et al., 2016; Campbell et al., 2017), barley (*Hordeum vulgare* L.) (Ward et al., 2019), and wheat (*Triticum aestivum L.*) (Lyra et al., 2020). In sorghum, HTPS have been implemented to study the relative growth rate in both belowground (Joshi et al., 2017) and aboveground organs (Gaillard et al., 2020; McCormick et al., 2016; Miao, Pages, et al., 2020; Neilson et al., 2015) under controlled environments. However, plant performance under controlled conditions is poorly correlated with crop performance in the target production environments (Poorter et al., 2016). Thus, deploying in-field HTPS is critical to generate new knowledge about the genetic control of canopy architecture.

Among the field-based HTPS deployed for studying sorghum, unmanned aerial vehicles (UAVs) have been widely utilized to study the dynamics of traits such as plant height (Hu et al., 2018; Pugh et al., 2018; Varela et al., 2021; Watanabe et al., 2017), leaf area index (Spindel et al., 2018), and biomass (Spindel et al., 2018; Varela et al., 2021). Nevertheless, UAVs are not effective in characterizing lower canopy layers, especially in late growing stages (Gage et al., 2019;

Sun et al., 2018). Therefore, ground-based systems capable of navigating through the canopy and equipped with side view sensors are preferred to unravel the variation in canopy architecture across their different levels (Xu & Li, 2022).

Several ground-based HTPS have been developed over the years. Small rovers have been implemented to describe canopy layers and latent space phenotypes in maize (Gage et al., 2019), whereas other systems have been used to study yield components in rice (Tanger et al., 2017), wheat (Jiang et al., 2018), and biomass accumulation in triticale (Busemeyer et al., 2013). In sorghum, ground-based HTPS have been deployed to study traits at lower layers, such as stem width (Jiang et al., 2018; Young et al., 2019) and leaf length (Vijayarangan et al., 2018). Furthermore, stem diameter (Salas Fernandez et al., 2017), plant width (Mantilla-Perez et al., 2020), plant height (Breitzman et al., 2019; Salas Fernandez et al., 2017), convex hull volume (CHV), and plant surface area (PSA) (Breitzman et al., 2019) have been studied using Phenobot 1.0 (Bao et al., 2019; Salas Fernandez et al., 2017). This ground-based HTPS was specifically designed to study canopy architecture in tall and densely planted crops such as biomass sorghum (Salas Fernandez et al., 2017). Phenobot 1.0 is equipped with stereo cameras capable of collecting 2D red, green, and blue images. Stereo images capture the same unit of information collected from two different angles (Salas Fernandez et al., 2017), which facilitates the 3D reconstruction of the canopy by matching the stereo images pixel by pixel (Bao et al., 2019). From the 3D canopy reconstruction, four image-derived descriptors of canopy architecture are extracted: plot-based plant height (PBPH), plot-based plant width (PBPW), CHV, and PSA (Bao et al., 2019). These canopy descriptors collected at the end of the season have been validated by comparing them with ground-truth phenotypes (Breitzman et al., 2019) and utilized for genome-wide association studies (GWAS). The genomic regions associated with variation in these image-derived canopy descriptors (Breitzman et al., 2019; Mantilla-Perez et al., 2020; Salas Fernandez et al., 2017) co-localized with those obtained using manual measurements (Mantilla-Perez et al., 2020; Olatoye et al., 2020; Zhao et al., 2016; Zhi, Massey-Reed, et al., 2022).

To date, field-based studies reporting sorghum growth rates have been focused primarily on plant height (Mu et al., 2022; Varela et al., 2021). Although natural genetic variation for canopy architecture at the end of the season has been reported (Bao et al., 2019; Breitzman et al., 2019; Mantilla-Perez et al., 2020), there is a knowledge gap in understanding the growth rate and canopy dynamics throughout the growing season.

In this project, we deployed Phenobot 1.0 to (i) collect four canopy architecture descriptors (PBPH, PBPW, PSA, and CHV) across the growing season in two diverse sorghum populations, (ii) determine the growth rates of these descriptors for each genotype, and (iii) investigate the genetic architecture of the four canopy descriptors at individual timepoints and their corresponding growth rates.

## 2 | MATERIALS AND METHODS

### 2.1 | Diversity panels

Two diverse sorghum populations representing the major cultivated races were utilized in this study: (i) the widely studied Sorghum Association Panel (SAP), comprising 325 photoperiod-insensitive accessions (Casa et al., 2008) and (ii) the Photoperiod-Sensitive Panel (PSP) that includes a set of 299 photoperiod-sensitive accessions (Yu et al., 2016). The PSP was assembled to represent the diversity of photoperiod-sensitive sorghum lines available in the National Plant Germplasm System (Yu et al., 2016).

### 2.2 | Experimental design and data acquisition

Both panels were planted in 2014 using a randomized complete block design with two replications at the Agricultural Engineering and Agronomy Research Farm (AEARF) in Boone, Iowa, on May 30 and at Curtiss Farm in Ames, Iowa, on June 12, aiming to maximize differences in environmental conditions between locations. Each experimental unit was a 3-m long two-row plot with 1.5-m inter-row spacing and 2.2-m inter-plot spacing. Because the SAP includes short grain-type and tall forage-type accessions, blocks were subdivided by sorghum type to reduce competition due to height differences.

### 2.3 | Phenotypic data acquisition

The Phenobot 1.0 platform (Bao et al., 2019; Salas Fernandez et al., 2017) was utilized to obtain stereo images as reported by Salas Fernandez et al. (2017). Briefly, Phenobot 1.0 navigated between the two-row plots collecting stereo images simultaneously from rows on each side. Data were obtained on July 18, July 24, July 30, and August 13 at AEARF, and July 18, August 4, August 14, and August 19 at Curtis Farm, corresponding to weeks 7, 8, 9, and 10 after planting (WAP). Stereo images were processed using the 3DMST algorithm (Bao et al., 2019; L. Li et al., 2017) to reconstruct 3D point clouds of the sorghum canopy. Subsequently, an axis-aligned bounding box (AABB) was fitted to the point cloud, with the $x$-axis parallel to the row height, the $y$-axis parallel to the row direction, and the $z$-axis perpendicular to the row direction (Figure S1). To eliminate the effect of outlier points on the estimation of descriptors, the AABB was partitioned into 20

equal slices across the *y*-axis, and each slice was weighted by calculating the ratio between the number of points in the slice and the total number of points in the plot. The maximum values on the *x*- and *z*-axes and the minimum value on the *z*-axis were determined for each slice, and then a weighted median was obtained for the entire plot. PBPH was extracted as the height from the ground to the top of the *x*-axis, whereas PBPW was determined as the width of the *z*-axis (Bao et al., 2019). For a given 3D point cloud, the convex hull is the smallest convex path containing all the points. This path was fitted for each slice, obtaining up to 20 convex hulls. A convex hull was considered valid if the ratio of its volume to the slice volume was ≥0.3, and only row images containing at least eight valid convex hulls were included in the analysis. CHV, which represents canopy volume, was obtained as the sum of all the valid individual convex hulls from each row (Figure S1B). Finally, a triangle mesh surface representation was fitted to the point cloud enclosing the outmost external layer of the canopy. PSA was calculated as the sum of the area of those triangles in the surface representation, including leaves, stems, and panicles (Figure S1C).

## 2.4 | Statistical analyses

Independent analyses were performed for each combination of population (PSP and SAP), date (7, 8, 9, 10 WAP), and canopy descriptor. Linear mixed models were fitted using the package *lme4* (Bates et al., 2015) in R (R Core Development Team, 2023) as follows:

$$Y_{ijk} = \mu + G_i + L_j + GL_{ij} + B_{(j)k} + \varepsilon_{ijk}, \quad (1)$$

where $Y_{ijk}$ is the response variable (i.e., canopy descriptor), $\mu$ is the overall mean, $G_i$ is the effect of the $i$th genotype, $L_j$ is the effect of the $j$th location, $GL_{ij}$ is the effect of the interaction between $i$th genotype and $j$th location, $B_{(j)k}$ is the effect of the $k$th block nested within the $j$th location, and $\varepsilon_{ijk}$ is the residual variable. All terms were treated as random effects, and the best linear unbiased predictor (BLUP) was obtained for each genotype.

Based on observed patterns of data across timepoints (Figure S2), linear models were fitted to estimate growth rates for each canopy descriptor because data were collected during the linear growth phase of the crop. Before model fitting, data were centered toward the midpoint of the analyzed growing window to avoid extrapolation on the intercept and provide a biological meaning. The four canopy descriptors were modeled as follows:

$$Y_{ijkm} = \mu + G_i + D_j + GD_{ij} + L_k + GL_{ik} + B_{(k)m} + \varepsilon_{ijkm}, \quad (2)$$

where $Y_{ijkm}$ is the response variable, $\mu$ is the overall mean, $G_i$ is the effect of the $i$th genotype, $D_j$ is the effect of the $j$th day after planting, $GD_{ij}$ is the interaction between the effect of $i$th genotype and $j$th day after planting, $L_k$ is the effect of the $k$th location, $GL_{ik}$ is the interaction effect between the $i$th genotype and the $k$th location, $B_{(k)m}$ is the effect of the $m$th block nested within the $k$th location, and $\varepsilon_{ijkm}$ is the residual variable. The terms $G_i$, $D_j$, and $GD_{ij}$ were treated as fixed effects, whereas the remaining terms were treated as random effects. $GD_{ij}$ represents the genotypic growth rate, whereas the intercept represents the genotypic value at the mid-point of the analyzed window (Figure 1). Both parameters were extracted using the package *emmeans* (Lenth et al., 2023).

Pearson correlation coefficients were computed using the *cor* procedure, and plots were generated using the package *corrplot* (Wei & Simko, 2021). Broad-sense heritability was calculated as (Carena et al., 2010) follows:

$$H^2 = \frac{\sigma^2_G}{\sigma^2_G + \frac{\sigma^2_{G\times E}}{n} + \frac{\sigma^2_e}{n\times r}}, \quad (3)$$

with $\sigma^2_G$ as the genotypic variance, $\sigma^2_{G\times E}$ as the variance of the genotype × environment interaction, $\sigma^2_e$ as the residual variance, and $n$ and $r$ as the number of locations and replications, respectively.

PBPH has been reported to be highly correlated with CHV and PSA (Breitzman et al., 2019; Salas Fernandez et al., 2017). Therefore, for the GWAS by timepoint, BLUPs for these traits were calculated using PBPH as a covariate. Plots and graphical representations were generated using the *ggplot2* library in R (Wickham et al., 2019).

## 2.5 | Genotypic data

The SAP was previously genotyped using genotyping-by-sequencing (GBS) and imputed according to Morris et al. (2013). A set of 165,241 single nucleotide polymorphisms (SNPs) was used after filtering for minor allele frequency (MAF) >15% and missing data <20%. For the analysis of the PSP, two genotypic sets were merged: (i) 157,000 SNPs generated by conventional genotyping-by-sequencing and imputed according to Yu et al. (2016) and (ii) 49,000 SNPs generated by tunable genotyping-by-sequencing (tGBS) (Ott et al., 2017). The genotypic dataset generated by tGBS was imputed using Beagle 4.1 (Browning & Browning, 2016). After filtering for MAF >0.15 and missing data <20%, a total of 126,664 SNPs were identified and used subsequently. For the combined GWAS analysis of SAP and PSP (PSP + SAP), only common SNPs across both panels were selected. A final set of 93,374 SNPs was utilized after filtering for missing data and MAF using the previously described criteria. All marker

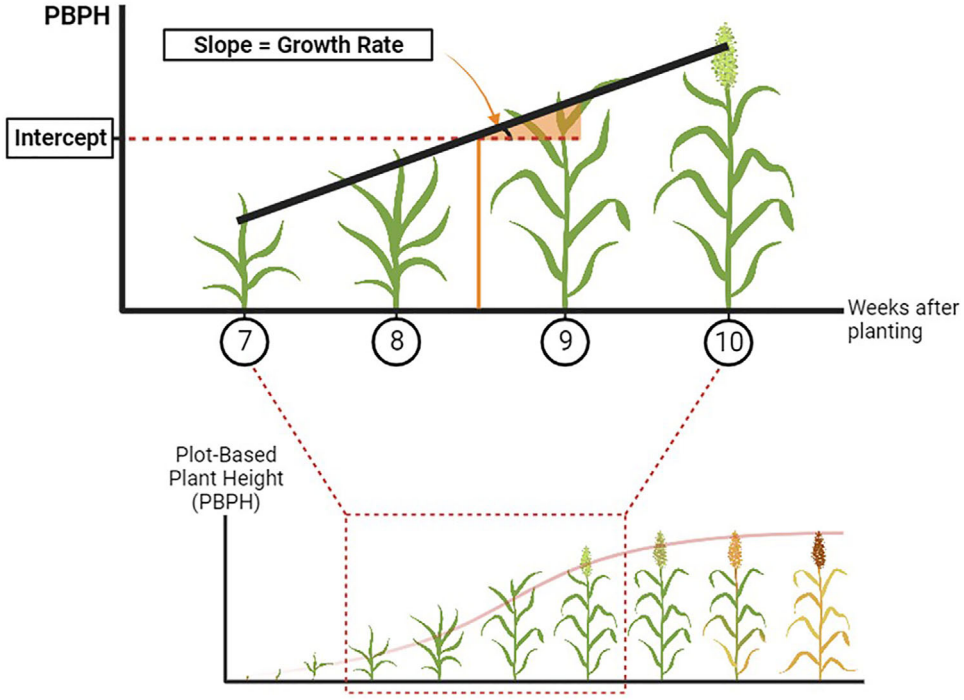


**FIGURE 1** Representation of the analyzed stages in each canopy descriptor using plot-based plant height (PBPH) as an example. The observed timepoints are indicated in circles, whereas the estimated parameters (growth rate and intercept) are in boxes. The diagram was generated using BioRender.com.

coordinates were named according to the Sorghum genome version 1.4.

## 2.6 | Population structure

The utilized Q matrix of population structure in the SAP was calculated in STRUCTURE 2.2.3 (Pritchard et al., 2000) as described in Mantilla Perez et al. (2014). To determine the population structure for the PSP, 263 SNPs separated by at least 350 kb and with less than 15% of missing data were randomly selected across the 10 sorghum chromosomes. STRUCTURE 2.3.4 software (Pritchard et al., 2000) was run with a 30,000 burn-in period, and 40,000 MCMC replicates. Sub-populations were assumed from 2 to 10, and 10 replicates of each assumed subpopulation number were performed. The optimal number of subpopulations was detected by implementing STRUCTURE Harvester (Earl & vonHoldt, 2012), looking for the smallest number of subpopulations maximizing DeltaK and minimizing the variation among runs. For the combined SAP and PSP panel (SAP + PSP), population structure was re-estimated with 765 SNPs and 2–10 subpopulations. All the software settings and criteria for selecting SNPs and the optimal number of populations were similar to those described for the PSP.

## 2.7 | Genome-wide association analysis

GWAS was performed in R using the FarmCPU implementation of GAPIT (X. Liu et al., 2016; J. Wang & Zhang, 2021). For the analysis of growth rates, since the *Dw1* and *Dw3* genes have a major role in plant height and leaf angle, markers linked to these genes were used as covariates when studying the SAP and SAP+PSP. The population structure matrix (Q) was utilized as a covariate to reduce the false positive associations due to population stratification. A false discovery rate threshold (Benjamini & Hochberg, 1995) of 0.05 was utilized to correct for multiple comparisons.

The search of candidate genes was focused on those regions associated with growth rates, which did not co-localize with known genes controlling canopy architecture (i.e., *Dw1*, *Dw2*, *Dw3*, *Ma1*, and *Ma6*). A window of 100 kb to each side of the significant SNPs was used for searching (i) candidate genes using the Sorghum genome version 3.1.1 and (ii) co-localizing QTL using the Sorghum QTL Atlas (Mace et al., 2019). Homologous genes of interest were identified by protein identity with other species using *PaperBLAST* (Price & Arkin, 2017). In summary, proposed candidate genes for future functional validations were identified based on the physical position of the significant marker, the function of homologous genes, and the co-localization

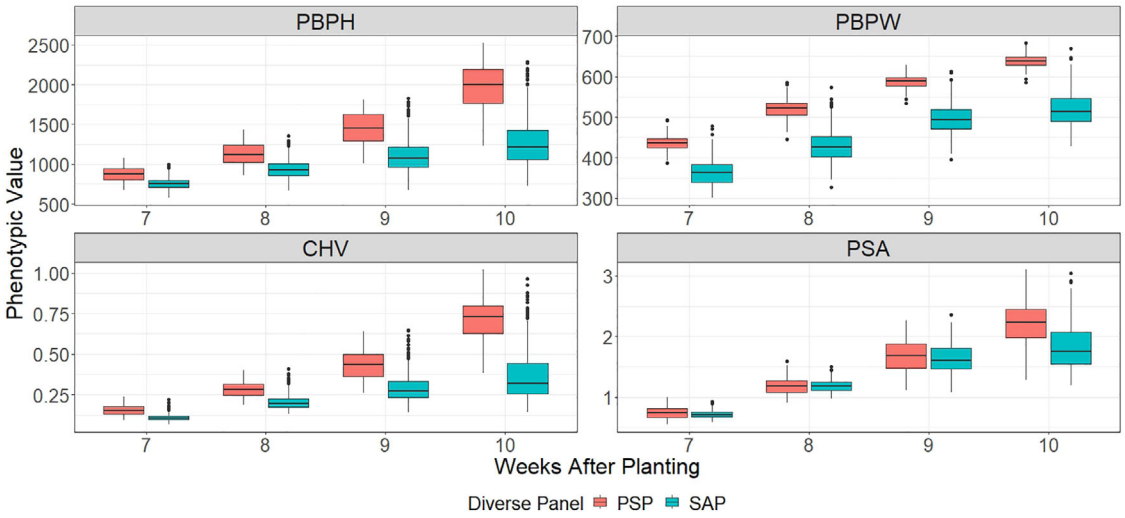


**FIGURE 2** Phenotypic variation of four canopy descriptors across the growing season for the Sorghum Association Panel (SAP) and Photoperiod-Sensitive Panel (PSP). CHV, convex hull volume [$m^3$]; PBPH, plot-based plant height [mm]; PBPW, plot-based plant width [mm]; PSA, plant surface area [$m^2$].

with QTL reported for similar or related traits on the Sorghum QTL Atlas.

## 3 | RESULTS

### 3.1 | Phenotypic analysis

#### 3.1.1 | Timepoint analysis

The means of the four canopy descriptors were consistently higher and increased more rapidly over time in the PSP than in the SAP (Figure 2). PBPH and CHV showed larger differences between populations compared to PBPW and PSA. In the last timepoint, the PSA mean was 15% higher in the PSP compared to the SAP (Table S1), whereas on previous dates, this canopy descriptor did not show differences between populations (Table S1). PBPW was 15%–18% higher in the PSP across all timepoints, but the range of variation was consistently larger in the SAP (Table S1). All traits showed significant genotype and genotype-by-environment (G × E) effects in both populations, except for CHV, PSA, and PBPW at 9 WAP, and PBPW at 10 WAP, which showed no significant G × E effects in the PSP (Table S2).

High and significant correlations were observed between PBPH and CHV ($r = 0.91$–$0.95$ for PSP, Figure S3, $r = 0.85$–$0.98$ for SAP, Figure S4) and between PBPH and PSA ($r = 0.79$–$0.91$ for PSP, $r = 0.85$–$0.90$ for SAP) across timepoints. PBPW showed the lowest correlation coefficients with PBPH, CHV, and PSA at all timepoints in both populations. Interestingly, these correlations have different trends between populations. While in the SAP (Figure S4), the magnitude of the correlation was similar across dates, in the PSP, the relationship between PBPW and other variables decreases over time ($r = 0.35$ to $-0.34$ for PBPH, $r = 0.5$ to $-0.24$ for CHV, and $r = 0.19$ to $-0.57$ for PSA) (Figure S3).

PBPH and CHV showed high and increasing heritability values over time (Table S3). In contrast, PBPW and PSA heritabilities exhibited varying patterns across populations, increasing over time in the SAP but remaining stable or slightly decreasing in the PSP. Additionally, PBPW showed consistently lower heritability in the PSP, suggesting a reduced genetic variation for this trait among genotypes that remained in the vegetative stage for the entire season.

#### 3.1.2 | Growth model

The parameters extracted through the growth model (i.e., intercept and growth rate) showed overall higher values in the PSP compared to the SAP (Figure 3), similar to the pattern observed in the timepoint analysis. Growth rates for PBPH and CHV were approximately doubled compared to those for the PSP (Table S4). PBPW was the only descriptor for which the intercept and growth rate were negatively (PSP, Figure S5) or weakly correlated (SAP, Figure S6). The parameters in the remaining canopy descriptors showed high correlations ($r > 0.7$) in both populations. When comparing growth rates between canopy descriptors, only PBPW showed negative correlations with all traits in the PSP, whereas in the SAP, it was only weakly correlated with CHV ($r = 0.14$).

A larger proportion of the total variance was explained by the genotype effect for growth rate descriptors than for the intercepts, with a small contribution of the G × E component (Figure S7). Although the residual component of the variance tended to be higher for the growth rates compared to the intercepts, in general, it was lower than the genotypic component, except for PBPW. In that case, the larger

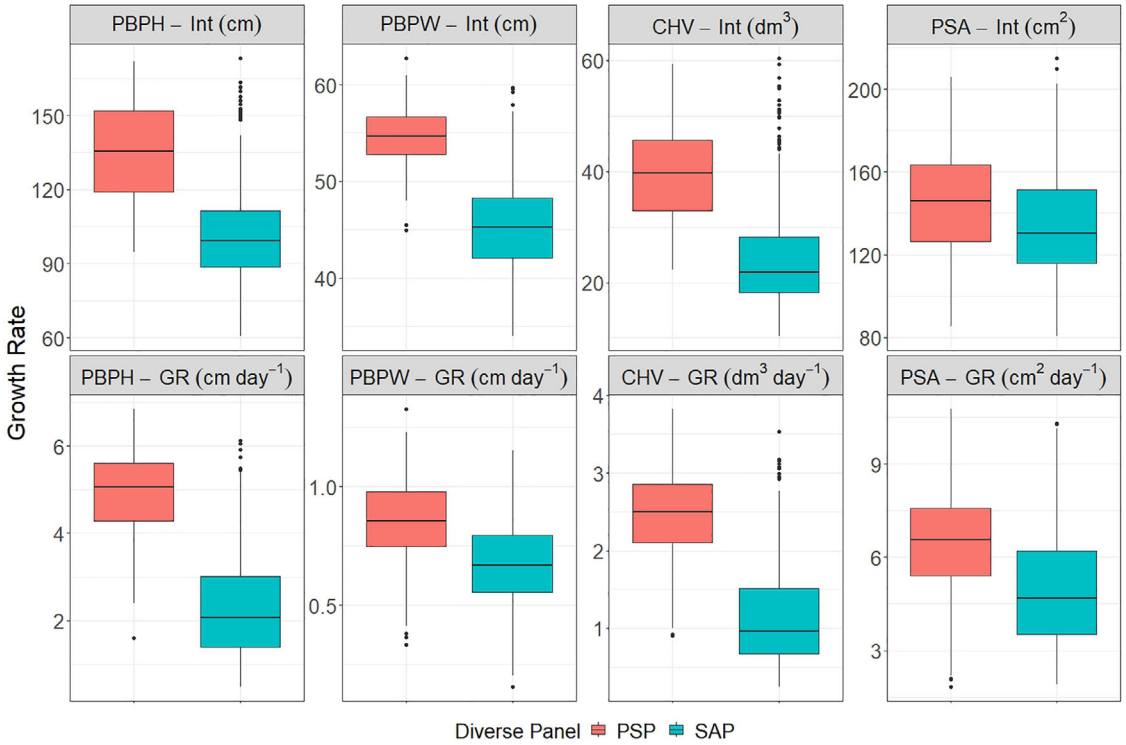


**FIGURE 3** Phenotypic variation in the centered intercept and growth rate for four canopy descriptors in the Sorghum Association Panel (SAP) and Photoperiod-Sensitive Panel (PSP). CHV, convex hull volume; GR, growth rate; Int, intercept; PBPH, plot-based plant height; PBPW, plot-based plant width; PSA, plant surface area.

proportion of unexplained variance was reflected in heritability values for the intercepts that were twice as large as for the growth rates (Table S3). Nevertheless, broad sense heritabilities were moderate-to-high for both parameters in the studied traits (Table S3).

## 3.2 | Genome-wide association analysis

### 3.2.1 | Population structure

The population structure analysis suggested $k = 4$ as the optimal number of subpopulations for the PSP in agreement with previous studies (Yu et al., 2016) and $k = 5$ subpopulations for the PSP + SAP. This difference between populations was expected considering that the SAP ($k = 5$ subpopulations) includes *kafir*, *durra*, *caudatum*, and the intermediate races *guinea/bicolor* and *guinea-caudatum* (Mantilla Perez et al., 2014), while the *kafir* group is underrepresented in the PSP (Yu et al., 2016).

### 3.2.2 | GWAS timepoint analysis

A total of 166 marker-trait associations (MTA) were discovered using the single population approach, 107 in the SAP and 59 in the PSP (Table 1, Figure S8). PBPH was the descriptor with the largest number of associations (80), followed by PBPW (35), CHV (26), and PSA (25). Among them, nine SNPs in the SAP and three SNPs in the PSP explained variation in a particular trait across dates or in multiple traits for the same date.

In the SAP, 93 out of 135 MTA were unique combinations of canopy descriptor, timepoint, and marker, responsible for 1.25%–16.81% of the phenotypic variance explained (PVE). The largest marker effects were detected for PBPH. For example, the SNP *S5_1702688* was responsible for 15.58% and 11.6% of the PVE at 7 and 8 WAP, respectively (Figure 4, Table S5, Figure S9). *S9_57240634* was significant at every timepoint, and its effect oscillated between 1.41% and 2.02% PVE across weeks. Three markers on chromosome 7 were associated with PBPW (*S7_58390037*) and PBPH (*S7_58576095*) across timepoints and with PBPH and CHV at 2 different weeks (*S7_58610000*). The SNPs *S6_42736415*, *S8_4621888*, and *S10_43199191* were discovered controlling PBPH at two timepoints, although they were responsible for small phenotypic variation (1.36%–3.00% PVE). As expected, based on abundant evidence of the role of *Dw3* in plant height and leaf angle determination, *S7_58610000*, a polymorphism in *Dw3* (Zhao et al., 2016), was significantly associated with PBPH at 10 WAP and CHV at 7 WAP (Figure 4, Table S5). The functional polymorphism of *Dw3* is an 882-bp tandem duplication in exon 5 (Multani et al., 2003), encoded as *S7_58610000*.

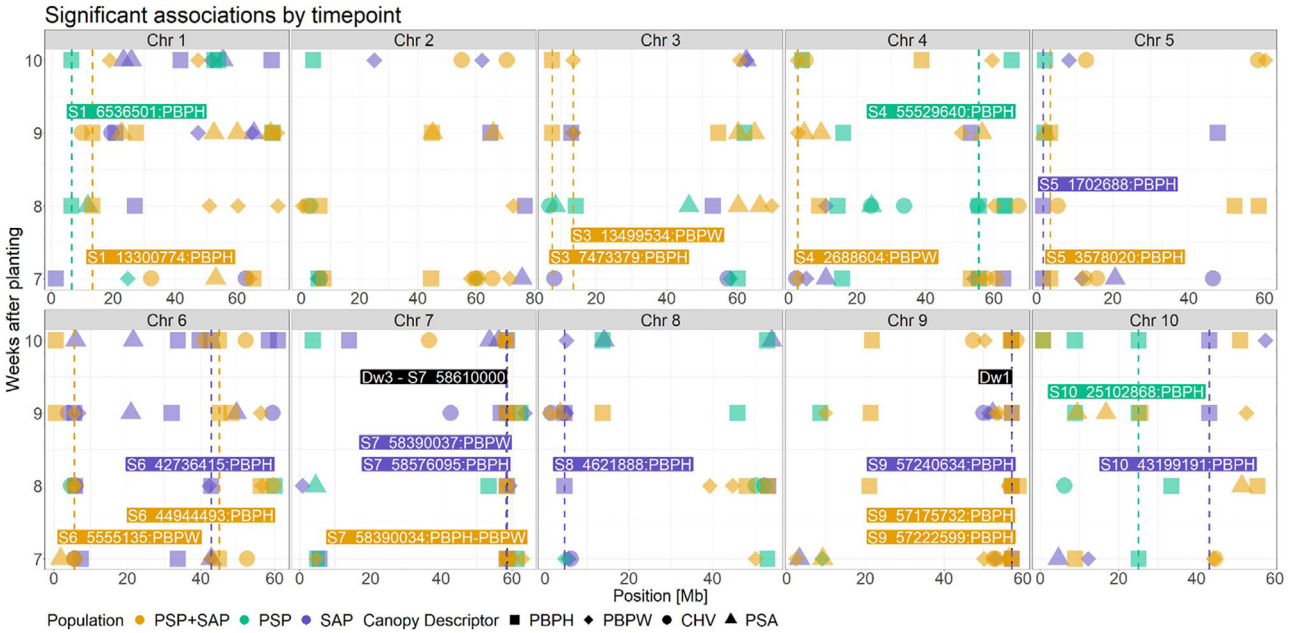


**FIGURE 4** Summary of the significant single nucleotide polymorphisms (SNPs) discovered in the genome-wide association analysis for four canopy descriptors at each timepoint in the Sorghum Association Panel (SAP), Photoperiod-Sensitive Panel (PSP), and combined analysis (PSP + SAP). SNPs associated with the same descriptor at different timepoints are indicated with vertical lines and color labeled according to population. The position of *Dw1* and the specific marker for *Dw3* are indicated in black. Chr, chromosome; CHV, convex hull volume; PBPH, plot-based plant height; PBPW, plot-based plant width; PSA, plant surface area.

In the PSP, 52 out of 59 MTA resulted in unique associations with PBPH, PBPW, CHV, and PSA. The range of variation explained (Table S5) by these unique MTA (1.32%–8.35%) was larger than that corresponding to the SNPs significant at multiple timepoints (1.53%–3.59%). Unlike the SAP, there were no major (>10% PVE) quantitative trait nucleotides (QTNs) detected in the PSP. Three SNPs (i.e., *S1_6536501*, *S4_55529640*, and *S10_25102868*) were associated with PBPH at multiple timepoints (Figure 4, Figure S9). Among them, *S10_25102868* was identified at three timepoints with a larger effect at 7 WAP (3.36% PVE) compared to 10 WAP (1.57% PVE).

### 3.2.3 | Combining photoperiod and non-photoperiod-sensitive populations for QTN detection

The combination of PSP and SAP (PSP + SAP) facilitated the discovery of 153 significant MTAs for PBPH (48), PBPW (50), CHV (33), and PSA (22) (Table 1). Most of them (114) were unique associations responsible for less than 5% PVE (Table S5), and 11 had moderate effects (5%–7.49% PVE). Ten SNPs were responsible for 28 MTA for PBPH and PBPW across timepoints (Figure 4, Figure S9) with a larger range of effects compared to unique associations (1.36%–10.21% PVE) (Table S5). The most consistent signals across time were in the vicinity of *Dw3* and *Dw1*, where *S7_58390034* was associated with PBPH and PBPW at every timepoint and *S9_57175732* and *S9_57222599* with PBPH at 7–8 and 9–10 WAP, respectively (Table S5). These SNPs had mostly small effects (1.36%–4.89% of the PVE) on the combined population analysis (Table S5). *S1_13300774* was associated with PBPH at 8–9 WAP with larger effects (3.63%–7.98% PVE) (Table S5). Other significant SNPs for PBPH at two (*S3_7473379*, *S5_3578020*) or three timepoints (*S6_44944493*) had a limited range of effects (1.36%–3.79% PVE), similar to *S3_13499534*, *S4_2688604*, and *S6_5555135*, associated with PBPW (1.44%–4.83% of the PVE) (Figure 4, Figure S9).

### 3.2.4 | Growth rate and intercept are under independent genetic control in both populations

Using no covariates (*Dw1* or *Dw3*), a total of 76 SNPs resulted in 90 MTAs for the intercepts and growth rates of all canopy descriptors, 27 in the PSP and 63 in the SAP (Table 2, Figures S10 and S11). This approach did not render any QTNs for the growth rate of PBPW in any population. A larger number of QTNs were detected for the intercepts than the growth rates (Table 2), and only five SNPs in the SAP were associated with both growth rate and intercept (Table S5).

In the PSP, five SNPs were discovered associated with PBPH growth rates (Figure 5). Two of them (*S2_13501075* and *S4_44244911*) showed small effects (1.83 and 1.52% PVE respectively), whereas *S4_65479629*, *S5_53109165*, and *S8_13750158* were responsible for 11.42%–12.26% of PVE

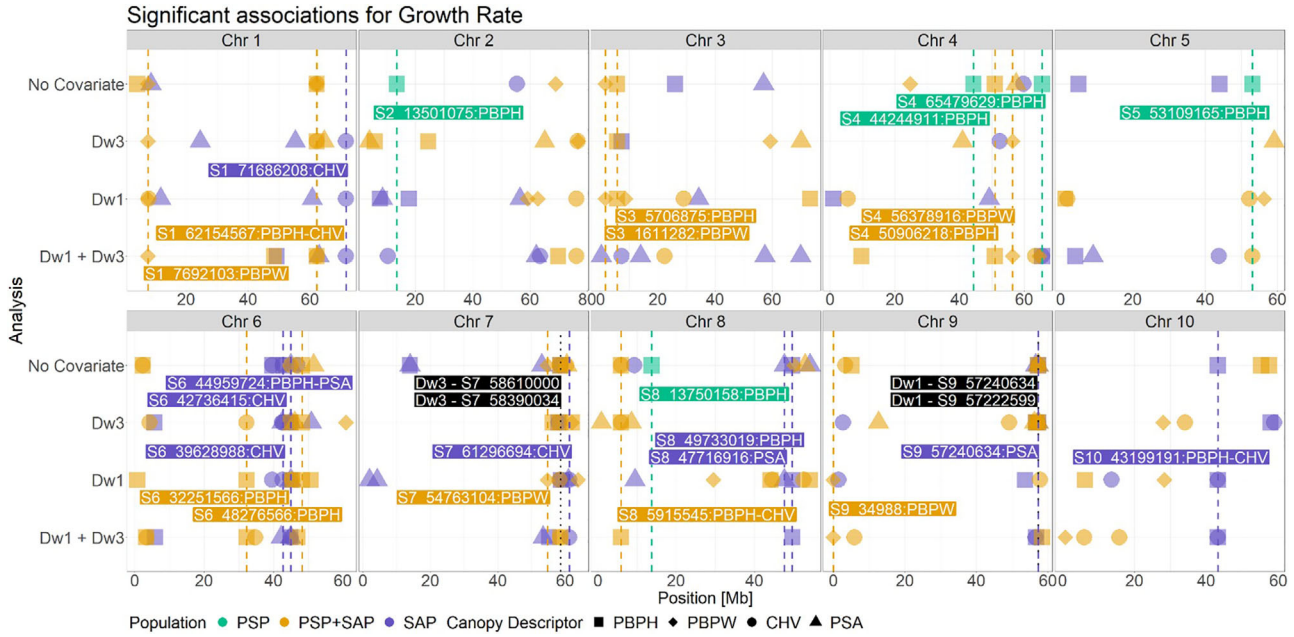


**FIGURE 5** Summary of the significant single nucleotide polymorphisms (SNPs) discovered in the genome-wide association analysis for growth rate of four canopy descriptors in the Sorghum Association Panel (SAP), Photoperiod-Sensitive Panel (PSP), and combined analysis (PSP + SAP). SNPs associated with the same descriptor using different analyses are indicated with vertical lines and color labeled according to population. Markers used as covariates for *Dw3* and *Dw1* genes are indicated in black. Chr, chromosome; CHV, convex hull volume; PBPH, plot-based plant height; PBPW, plot-based plant width; PSA, plant surface area.

(Table S5). All QTNs in the PSP resulted in unique MTA unlike the SAP, where seven SNPs accounted for 33% of the QTNs (Figure 5, Table S5).

In the SAP, as observed in the timepoint analysis, markers representing *Dw3* (*S7_58610000*) and *Dw1* (*S9_57240634*) showed the strongest associations with both growth rates and intercepts for CHV and PBPH (*Dw3*), and CHV and PSA (*Dw1*) (Table S5). The SNPs *S6_39628988*, *S6_44959724*, and *S10_43199191* were associated with both parameters for CHV, PSA, and PHPB, respectively, having moderate effects (2.55%–4.53%) (Table S5). These five markers were the only ones having simultaneous signals for growth rate and intercept in the analysis without covariates.

Given the large effects of the *Dw3* and *Dw1* genes in the SAP, the GWA analysis was also performed using *S7_58610000* and *S9_57240634* as covariates. As expected, some QTN signals on chromosomes 7 and 9 disappeared when the nearby gene was used as a covariate (Figure 5, Table S5). The analysis with covariates facilitated the discovery and validation of QTNs for growth rates that were not related to the major dwarfing genes (Figure 5). While the use of covariates enabled the detection of *S1_71686208* (CHV), *S6_44959724* (PBPH), and *S10_43199191* (CHV), this approach contributed to validate QTNs detected without covariates, such as *S6_42736415* (CHV), *S6_44959724* (PSA), *S8_47716916* (PSA), *S8_49733019* (PBPH), and *S10_43199191* (PBPH). Like the analysis without covariates, only two (with *Dw3* as a covariate) and three (with *Dw1* and *Dw1+Dw3* as covariate) SNPs were controlling growth rate and intercepts simultaneously, representing less than 20% of the MTAs (Tables S5).

### 3.2.5 | Combining populations facilitates the detection of novel regions associated with growth rates

In the PSP + SAP analysis, 68 MTAs were identified for all possible combinations of parameters and canopy descriptors without using covariates (Table 2). In the vicinity of *Dw3*, *S7_58390034* was detected for both growth rate and intercept of CHV, and controlling only the intercepts of PBPH, PBPW, and PSA. The marker representing *Dw1* in the PSP + SAP analysis, *S9_57222599*, was associated with both parameters for PBPH, CHV, and PSA. Since *S7_58390034* and *S9_57222599* were the closest SNPs to *Dw3* and *Dw1*, respectively, these were used as covariates in subsequent analyses.

*Dw1* and *Dw3* were used as covariates in the analysis to either validate markers in the vicinity of these genes that could represent novel QTNs or increase the power to discover new MTAs with smaller effects. For example, the use of *Dw3* as a covariate increased the number of QTNs by 11% relative to the analysis without covariates,

**TABLE 1** Number of significant marker-trait associations detected in the genome-wide association analysis using the Sorghum Association Panel (SAP), the Photoperiod-Sensitive Panel (PSP), and the combined analysis merging the two populations (PSP + SAP).

| Canopy descriptor | WAP | SAP | PSP | PSP + SAP |
|---|---|---|---|---|
| PBPH | | | | |
| | 7 | 8 | 8 | 9 |
| | 8 | 10 | 9 | 13 |
| | 9 | 12 | 9 | 16 |
| | 10 | 11 | 13 | 10 |
| PBPW | | | | |
| | 7 | 9 | 6 | 16 |
| | 8 | 4 | | 13 |
| | 9 | 8 | | 12 |
| | 10 | 8 | | 9 |
| CHV | | | | |
| | 7 | 9 | | 15 |
| | 8 | 1 | 9 | 6 |
| | 9 | 7 | | 1 |
| | 10 | | | 11 |
| PSA | | | | |
| | 7 | 6 | | 4 |
| | 8 | | 5 | 3 |
| | 9 | 4 | | 15 |
| | 10 | 10 | | |
| Total | | 107 | 59 | 153 |

Abbreviations: CHV, convex hull volume; PBPH, plot-based plant height; PBPW, plot-based plant width; PSA, plant surface area.

including *S6_32251566*, which was detected for the growth rates and intercepts of PBPH, PBPW, and CHV (Table S5). Markers validated with and without covariates include (i) *S3_5706875*, which showed the largest effect controlling PBPH growth rate (10.55% PVE); (ii) *S1_62154657* and *S8_5915545* explaining variation in PBPH and CHV growth rate; and (iii) *S4_50906218* associated with PBPH growth rate (Table S5).

Merging the populations uncovered QTNs for PBPW growth rate that were not identified under the single population analysis (Figure 4, Table S5). Four QTNs were of particular interest because they were discovered to be associated with PBPW growth rate in more than one analysis: (i) *S1_7692103* and *S3_1611282* were significant with and without covariates and (ii) *S4_56378916* and *S9_34988* were detected in two analyses with covariates. However, none of the QTNs were associated with the PBPW intercept, suggesting an independent control of these parameters.

# 4 | DISCUSSION

The deployment of Phenobot 1.0 facilitated the study of canopy architecture dynamics at a large scale alleviating the "phenotyping bottleneck" (Furbank & Tester, 2011). This goal was achieved by decomposing the complex and longitudinal traits into biologically meaningful canopy descriptors (Bao et al., 2019; Breitzman et al., 2019).

In the SAP, heritabilities for the four canopy descriptors were similar to those previously reported for the same traits at the end of the growing season (Breitzman et al., 2019). The PSP showed smaller increases in heritability values over time compared to the SAP. In general, the PSP exhibited a larger initial growth that corresponds to the larger biomass accumulation occurring in bioenergy materials relative to grain types (Olson et al., 2012). Therefore, fast-growing genotypes in the PSP could have enlarged the genotypic differentiation among lines early in the season. This differentiation is exacerbated later among lines of the SAP, because of diversity in flowering time. While some genotypes might develop longer internodes early on, others could accumulate sugars in the stem for a longer period before initiating stem elongation, leading to genotypic differences in growth rate dynamics and canopy architecture.

## 4.1 | Major dwarfing genes influence crop growth rate

Regions co-localizing with the major dwarfing (*Dw*) genes *Dw2*, *Dw3*, and *Dw1* (P. J. Brown et al., 2008; J. Hilley et al., 2016; J. L. Hilley et al., 2017) have been previously associated with biomass accumulation in sorghum (Breitzman et al., 2019; Spindel et al., 2018), which were confirmed herein using HTP-derived descriptors to characterize the growth rate. *Dw3* is an auxin transporter that controls not only plant height but also leaf angle (Mantilla-Perez & Salas Fernandez, 2017; Truong et al., 2015). The specific marker for the tandem duplication in *Dw3* (*S7_58610000*) and neighboring SNPs (*S7_58576095*, *S7_58390034*) were consistently detected in the GWAS for growth rates and multiple timepoints. *Sobic.007G160400* is a zinc finger homeodomain 2 (ZFHD2) transcription factor localized 94.1 kb away from *S7_58390034*, which was consistently associated with PBPW during the growing season in the single timepoint analysis and its growth rate. This candidate gene, close to *Dw3*, has been previously reported to control PBPW at the end of the growing season (Breitzman et al., 2019) and the leaf angle of the upper canopy layer (Natukunda et al., 2022; Zhao et al., 2016).

*Dw1* (*Sobic.009G229800*) encodes a membrane protein involved in the regulation of cell proliferation, affecting

**TABLE 2** Number of significant marker-trait associations detected in the genome-wide association analysis for the intercept and growth rate of each canopy descriptor in the Sorghum Association Panel (SAP), the Photoperiod-Sensitive Panel (PSP), and the combined analysis (PSP + SAP).

| | No covariate | | | Covariate *Dw1* | | Covariate *Dw3* | | Covariate *Dw1* + *Dw3* | |
|---|---|---|---|---|---|---|---|---|---|
| | PSP | SAP | PSP + SAP | SAP | PSP + SAP | SAP | PSP + SAP | SAP | PSP + SAP |
| **PBPH** | | | | | | | | | |
| Intercept | 12 | 13 | 7 | 8 | 13 | 6 | 13 | 8 | 10 |
| Growth rate | 5 | 10 | 12 | 8 | 11 | 7 | 12 | 9 | 11 |
| **PBPW** | | | | | | | | | |
| Intercept | | 8 | 8 | 6 | 3 | 5 | 7 | 7 | 14 |
| Growth rate | | | 7 | | 11 | | 7 | | 5 |
| **CHV** | | | | | | | | | |
| Intercept | 1 | 11 | 11 | 8 | 10 | 10 | 6 | 8 | 10 |
| Growth rate | | 8 | 8 | 8 | 11 | 9 | 8 | 10 | 11 |
| **PSA** | | | | | | | | | |
| Intercept | 9 | 4 | 10 | 10 | | 4 | 11 | 6 | |
| Growth rate | | 9 | 5 | 12 | | 6 | 12 | 10 | |
| **Total** | 27 | 63 | 68 | 60 | 59 | 47 | 76 | 58 | 61 |

Abbreviations: CHV, convex hull volume; PBPH, plot-based plant height; PBPW, plot-based plant width; PSA, plant surface area.

internode length (J. Hilley et al., 2016; Yamaguchi et al., 2016). Plant height QTLs have been widely reported in this region at maturity (Bouchet et al., 2017; Felderhoff et al., 2012; Higgins et al., 2014) and at panicle emergence in a time-series GWAS (Miao, Xu, et al., 2020). The region of *Dw1* has also been previously associated with PBPH, PSA, and CHV at the end of the season (Breitzman et al., 2019). The relevance of *Dw1* in sorghum growth was validated in our study by detecting this association with PBPH growth rate in the SAP and the PSP + SAP analysis. Additionally, it was associated with variation in PBPH at every timepoint, confirming the effect exerted throughout the growing season.

## 4.2 | Proposed candidate genes within novel genomic regions controlling growth rate

### 4.2.1 | Chromosome 1

In this study, *S1_62154567* has been consistently associated with PBPH and CHV growth rates across multiple analyses. *S1_62154567* is in the second exon of *Sobic.001G409100*, which encodes a glycosyltransferase from family 43 (GT43) homologous to *T. aestivum* M5EF78 (71% identity), *Asparagus officinalis AJF38258* (48% identity), and *Arabidopsis thaliana IRX9* (41% identity). The GT43 family encompasses xylan xylosyltransferases that are involved in xylan biosynthesis in the Golgi lumen (Curry et al., 2023). Xylans are the second most important structural polysaccharides, reaching about 20% of the cell wall in grasses (Scheller & Ulvskov, 2010). GT43 proteins have been associated with rapid stem elongation in *Phyllostachys edulis* (Z. Li et al., 2021), straw digestibility in *Brachypodium distachyon* (Whitehead et al., 2018), and expansion of the xylan backbone in *T. aestivum* (Chateigner-Boutin et al., 2015; Lovegrove et al., 2013), *A. thaliana* (Lee et al., 2012; Wu et al., 2010), and *A. officinalis* (Zeng et al., 2016). Therefore, *Sobic.001G409100* constitutes an interesting candidate gene for future functional validation studies to improve sorghum growth rates by leveraging the role of xylan biosynthesis on biomass accumulation.

### 4.2.2 | Chromosome 3

The SNP *S3_5706875*, associated with PBPH growth rate, is ~25 kb from previously reported QTL for morphological traits such as panicle length and leaf area (Morris et al., 2013; Phuong et al., 2013), and ~50 kb from another QTL controlling photosynthetic capacity (Ferguson et al., 2021). Although *S3_5706875* is located in the first exon of *Sobic.003G066000*, low identity homologs were found in *A. thaliana* (*At5g01150*, 26% identity) and *Trifolium pratense* (*At5g01140*, 25% identity). Therefore, one of the most promising candidate genes is *Sobic.003G064800*, located 45 kb upstream from *S3_5706875* and encoding a dirigent (DIR)-like protein (Table 3). The *A. thaliana* homologous ESB1/AtDIR10 (55% identity) has been reported as being responsible for the formation of the casparian strip formation (Hosmani et al., 2013), affecting water use efficiency and therefore, wet biomass accumulation (Baxter et al., 2009). DIR proteins are critical for lignin biosynthesis (Paniagua et al., 2017) and are responsible for targeting precursor coniferyl alcohol to the lignification initiation sites such as the secondary walls of tracheary elements (Davin & Lewis, 2000).

**TABLE 3** Proposed candidate genes for the markers associated with growth rates of canopy descriptors.

| SNP | Position (v 3.1) | Population | Descriptor (analysis) | Candidate genes | Proposed candidate gene | Predicted function |
|---|---|---|---|---|---|---|
| *S1_62154567* | 69276608 | PSP + SAP | PBPH: growth rate (no covariate, *Dw3*, *Dw1+Dw3*)<br>CHV: growth rate (no covariate, *Dw3*, *Dw1+Dw3*) | 38 | *Sobic.001G409100* | Glucoronosyltransferase |
| *S3_5706875* | 5630891 | PSP + SAP | PBPH: growth rate (no covariate, *Dw1*, *Dw3*) | 43 | *Sobic.003G064800* | Dirigent-like protein |
| *S4_44244911* | 44838196 | PSP | PBPH: growth rate (no covariate) | 4 | *Sobic.004G145500* | Inositol polyphosphate-related phosphatase domain-containing protein |
| *S4_50906218* | 51607952 | PSP + SAP | PBPH: growth rate (no covariate, *Dw1+Dw3*) | 19 | *Sobic.004G166500* | N-carbamoylputrescine amidase |
| *S4_56378916* | 57051771 | PSP + SAP | PBPW: growth rate (*Dw3*, *Dw1xDw3*) | 17 | *Sobic.004G220300* | Phenylalanine ammonia-lyase |
| *S5_53109165* | 62646115 | PSP | PBPH: growth rate (no covariate) | 22 | *Sobic.005G154850* | NADP-dependent malic enzyme |
| | | | | | *Sobic.005G155900* | Uncharacterized protein |
| *S8_47716916* | 55062657 | SAP | PSA: growth rate (no covariate, *Dw1*) | 15 | *Sobic.008G126200* | Calmodulin-binding protein |
| *S9_34988* | 27820 | PSP + SAP | PBPW: growth rate (*Dw1*, *Dw1xDw3*) | 14 | *Sobic.009G000300* | Serine/threonine-protein kinase |

Abbreviations: CHV, convex hull volume; PBPH, plot-based plant height; PBPW, plot-based plant width; PSA, plant surface area; SNP, single nucleotide polymorphism.

### 4.2.3 | Chromosome 4

The marker *S4_44244911*, associated with PBPH growth rate in the PSP, co-localizes with several QTLs that explained variation in plant height (Bouchet et al., 2017; Shiringani et al., 2010), panicle length (Witt Hmon et al., 2014), and panicle exertion (Felderhoff et al., 2012). The identification of candidate genes in these previous studies has been difficult due to the large QTL interval (3–10 Mb). *S4_44244911* is in the first intron of *Sobic.004G145500*, predicted to encode an inositol polyphosphate phosphatase. The *A. thaliana* homologous *FRA3* (52% identity) was highly expressed in fiber cells in stems, influencing actin organization and secondary wall synthesis (Zhong et al., 2004), similar to the rice homolog *Dwarf50* (*D50*) (Sato-Izawa et al., 2012). *Z. mays Brevis plant1* (*Bv1*) is a gene closely related to *D50* and *FRA3*, which influences internode length by regulating the length of parenchyma cells without altering flowering time (Avila et al., 2016). *bv1* mutants showed the altered regulation of genes encoding cell wall and cytoskeleton-associated proteins. *Bv1* (Y. Chen et al., 2017), *FRA3* (Zhong et al., 2004), and *D50* (Sato-Izawa et al., 2012) are type II inositol polyphosphate 5-phosphatases. Their function is to hydrolyze phosphoinositides, which are signaling molecules regulating cellular functions such as cell differentiation, cell proliferation, and actin cytoskeleton organization (Takenawa & Itoh, 2001; Whisstock et al., 2002).

The SNP *S4_50906218*, significant for PBPH growth rate in the SAP+PSP analysis, falls within previous QTLs associated with regrowth (Paterson et al., 1995), plant height (Phuong et al., 2013), green leaf area (Haussmann et al., 2002), and leaf weight (Kapanigowda et al., 2014). This SNP is in the fourth exon of *Sobic.004G166500* with a predicted function of a carbamylputrescine amidase protein. Homologous genes in *A. thaliana NLP1* (80% identity), *Solanum lycopersicum NLP1* (81% identity), and *Medicago truncatula* MtCPA (81% identity) have been described catalyzing the hydrolysis of N-carbamoyl putrescine to putrescine in

the polyamine biosynthesis pathway (Piotrowski et al., 2003; Sekula et al., 2016). Polyamines are a type of growth regulators (D. Chen et al., 2019) and were found to promote floral development in *A. thaliana* (Applewhite et al., 2000). In sorghum, this candidate gene was reported in previous studies associated with the response to osmotic stress (Ngara et al., 2018) and dhurrin metabolism during grain development (Nielsen et al., 2016).

The SNP *S4_56378916* overlaps with QTL detected for dry biomass (Murray et al., 2009), stem diameter (Zou et al., 2012), and plant height (Mocoeur et al., 2015; Nagaraja Reddy et al., 2013). This marker is located in the first exon of *Sobic.004G220300*, the sorghum gene *SbPAL1* that encodes a phenylalanine ammonia-lyase (Jun et al., 2018). Enzymes from the PAL family are involved in the phenylalanine deamination in synthesis of *p*-coumarate, a precursor in the biosynthesis of lignin monomers (Zhang & Liu, 2015). A PAL knockdown in *B. distachyon* resulted in 43% reduction in lignin content in stem cell walls, showing better saccharification yield compared to the wild type (Cass et al., 2015). It was hypothesized that the modification of PAL activity could increase biomass conversion in grasses (Jun et al., 2018). Although PAL enzymes in monocots can also use tyrosine as a substrate (Barros et al., 2016; Cass et al., 2015; Rosler et al., 1997), in a biochemical characterization study, *SbPAL1* was demonstrated to have strong phenylalanine ammonia-lyase activity (Jun et al., 2018).

### 4.2.4 | Chromosome 5

The PSP facilitated the detection of *S5_53109165*, associated with PBPH growth rate. This SNP colocalizes with a QTL for plant height reported in the Nested Association Mapping population (Bouchet et al., 2017), whereas another study reports three QTLs for chlorophyl fluorescence and leaf appearance rate 32.8 kb from it (Fiedler et al., 2014). *S5_53109165* is in an intergenic region, and *Sobic*.005G154850 is the closest candidate gene (7.2 kb away). This gene encodes a malic enzyme (ME) homologous to NADP-ME in *A. thaliana* (88% identity), *O. sativa* (92% identity), and *Z. mays* (82% identity). NADP-ME catalyzes the oxidative decarboxylation of malic acid to pyruvic acid and carbon dioxide, reducing NADP (Drincovich et al., 2001; Edwards & Andreo, 1992). In *A. thaliana*, a reduced activity of NADP-ME switches the use of malic acid to oxaloacetate in the tri carboxylic acid cycle, promoting gluconeogenesis (N. J. Brown et al., 2010).

Another candidate gene, *Sobic.005G155900*, is located 81.6 kb from the significant marker and encodes an uncharacterized protein homologous to the *Z. mays* transcription factor *ZmMYB69* (47% identity). The overexpression of *ZmMYB69* resulted in reduced plant height in *Z. mays* (Qiang et al., 2022). This gene represses lignin biosynthesis through the activation of *ZmMYB31* and *ZmMYB42* (Qiang et al., 2022). The overexpression of these two genes in *A. thaliana* caused 60%–70% reduction in lignin content (Fornalé et al., 2010; Sonbol et al., 2009).

### 4.2.5 | Chromosome 8

The SNP *S8_47716916*, explaining variation in PSA growth rate, is colocalized with previous QTLs associated with biomass and leaf area (Mace et al., 2012; Spindel et al., 2018), stem diameter (J. Wang et al., 2022), tiller number (Zhao et al., 2016), panicle exertion (Felderhoff et al., 2012), and plant height (Phuong et al., 2013). Since PSA is a descriptor encompassing all plant organs (Breitzman et al., 2019), it includes vegetative and reproductive components of the canopy structure. Among the candidate genes, *Sobic.008G126200* is located at 47.6 Mb (55.01 Mb in v3.1) and encodes a calmodulin-binding protein-like, a family of ubiquitous proteins involved in calcium signaling and growth (Hepler, 2005; L. Wang et al., 2023). The *A. thaliana* calmodulin-binding kinase PSKR1 is responsible for growth signaling, showing a retardation in growth when the gene was knocked down (Hartmann et al., 2014). In addition, the closest homolog to the sorghum *Dw2* in *A. thaliana* is a kinesin-like calmodulin-binding protein kinase (J. L. Hilley et al., 2017), which interacts with other types of calmodulin-binding proteins to modulate the organization of cytoskeletal components (Day et al., 2000) and root growth (Humphrey et al., 2015).

### 4.2.6 | Chromosome 9

On a dynamic QTL mapping, a region ~10 bp away from *S9_34988* was detected associated with plant height during the early season (Miao, Xu, et al., 2020). In our study, this SNP explained variation in the growth rate of PBPW and overlaps with QTL for dry matter growth rate, leaf growth rate (Fiedler et al., 2014), total dry biomass, and dry leaf weight (Kapanigowda et al., 2014). The proposed candidate gene *Sobic.009G000300* encodes a serine/threonine protein kinase homologous to PERK8 in *A. thaliana* (58% identity), 26 kb away from the significant SNP. Members of the Proline-Rich Extensin-like Receptor Kinase (PERK) gene family interact with kinesin-like calmodulin-binding protein-interacting protein kinase to modulate growth (Humphrey et al., 2015). *Sobic.009G000300* gene was expressed in sorghum internodes (J. L. Hilley et al., 2017), and it has been hypothesized that PERK genes could interact with *Dw2* to regulate growth and the flow of cellular components during organ development (J. L. Hilley et al., 2017).

In summary, the genetic architecture of dynamics of PBPH, PBPW, CHV, and PSA across the season showed a

polygenic basis, that is, several genes controlling these traits with small-to-moderate effects. In the SAP, *Dw1* and *Dw3* have a significant role in the genetic control of growth rates, which was not observed in the PSP. The nature of the populations (Casa et al., 2008; Yu et al., 2016) is the likely cause of this discrepancy, since *Dw1* and *Dw3* are two major dwarfing genes utilized in sorghum breeding, and thus, with more noticeable effects in the SAP. By using growth rates as a phenotype, we were able to identify unique regions, not detected via the timepoint analysis. Additionally, the newly proposed candidate genes for growth rates encode mostly genes involved in the biosynthesis of lignin (*Sobic.003G064800* and *Sobic.005G155900*), lignin precursors (*Sobic.004G220300*), structural components of the cell wall (*Sobic.001G409100* and *Sobic.004G145500*), and growth regulators (*Sobic.004G166500*, *Sobic.008G126200*, and *Sobic.009G000300*). Based on their homology and known function in other species, these genes are promising candidates for functional validation and future targets in breeding pipelines.

## 5 | CONCLUSIONS

Crop growth is a complex and dynamic process, and the use of high-throughput phenotyping resources can ease the understanding of its genetic control by partitioning the trait into smaller components. In this study, we were able to deploy a field-based phenotyping platform to characterize two populations throughout the growing season, using canopy descriptors correlated with morphological parameters for canopy architecture. In addition, we unraveled genotypic differences in growth rates, leading to the identification of genomic regions contributing to canopy growth. While traits such as plant height have been widely studied in sorghum, this research provides novel information on canopy growth under field conditions. The genomic regions discovered through GWA, after functional validation, represent novel resources for sorghum breeding programs aiming to increase biomass. This new knowledge could be leveraged to characterize germplasm, facilitating the selection of lines to create new populations, and develop molecular markers for assisted selection in order to accelerate genetic gain.

## AUTHOR CONTRIBUTIONS

**Juan Panelo**: Data curation; formal analysis; investigation; visualization; writing—original draft. **Yin Bao**: Formal analysis; methodology; resources; software; validation; writing—review and editing. **Lie Tang**: Conceptualization; funding acquisition; investigation; methodology; resources; software; supervision; writing—review and editing. **Patrick Schnable**: Conceptualization; funding acquisition; project administration; resources; writing—review and editing. **Maria Salas-Fernandez**: Conceptualization; funding acquisition; investigation; project administration; resources; supervision; writing—original draft; writing—review and editing.

## ACKNOWLEDGMENTS

We thank Lisa Coffey (Schnable lab) and Nicole Lindsey (Salas-Fernandez lab) for their assistance in designing and conducting the field experiments with Phenobot 1.0. We also recognize Dr. Jianming Yu and Dr. Xiaran Li for sharing seeds and genotypic data of the PSP panel, and Eddy Yeh (Schnable lab) for providing the tGBS data for the PSP. This work was supported by the National Institute of Food and Agriculture, United States Department of Agriculture (grant number 2012-67009-19713) and the Plant Sciences Institute at Iowa State University. Maria G. Salas-Fernandez was also supported by the United States Department of Agriculture, National Institute of Food and Agriculture (grant number IOW04314).

## CONFLICT OF INTEREST STATEMENT

Patrick Schnable is a co-lead of the Genomes to Fields Initiative and PI of the USDA-NIFA funded Agricultural Genome to Phenome Initiative. He is a co-founder of Data2Bio, LLC; Dryland Genetics, Inc; and EnGeniousAg, LLC. He is a member of the scientific advisory boards of Kemin Industries and Centro de Tecnologia Canavieira. He is a recipient of research funding from Iowa Corn and Bayer Crop Science.

## DATA AVAILABILITY STATEMENT

Raw phenotypic data for canopy descriptors and R codes used for figures can be accessed at https://github.com/sorghum21/Panelo-etal-Genetics-of-canopy-architechture-dynamics. The genotypic dataset used for the SAP is available in Morris et al. (2013), whereas the genotypic dataset used for the PSP is available in Yu et al. (2016).

## ORCID

*Juan S. Panelo* https://orcid.org/0000-0002-0075-0157
*Maria G. Salas-Fernandez* https://orcid.org/0000-0001-6653-3385

## REFERENCES

Al-Tamimi, N., Brien, C., Oakey, H., Berger, B., Saade, S., Ho, Y. S., Schmöckel, S. M., Tester, M., & Negrão, S. (2016). Salinity tolerance loci revealed in rice using high-throughput non-invasive phenotyping. *Nature Communications*, *7*(1), 13342. https://doi.org/10.1038/ncomms13342

Applewhite, P. B., Kaur-Sawhney, R., & Galston, A. W. (2000). A role for spermidine in the bolting and flowering of *Arabidopsis*. *Physiologia Plantarum*, *108*(3), 314–320. https://doi.org/10.1034/j.1399-3054.2000.108003314.x

Avila, L. M., Cerrudo, D., Swanton, C., & Lukens, L. (2016). *Brevis plant1*, a putative inositol polyphosphate 5-phosphatase, is required

for internode elongation in maize. *Journal of Experimental Botany*, *67*(5), 1577–1588. https://doi.org/10.1093/jxb/erv554

Bao, Y., Tang, L., Breitzman, M. W., Salas Fernandez, M. G., & Schnable, P. S. (2019). Field-based robotic phenotyping of sorghum plant architecture using stereo vision. *Journal of Field Robotics*, *36*(2), 397–415. https://doi.org/10.1002/rob.21830

Barros, J., Serrani-Yarce, J. C., Chen, F., Baxter, D., Venables, B. J., & Dixon, R. A. (2016). Role of bifunctional ammonia-lyase in grass cell wall biosynthesis. *Nature Plants*, *2*(6), 16050. https://doi.org/10.1038/nplants.2016.50

Bates, D., Mächler, M., Bolker, B., & Walker, S. (2015). Fitting linear mixed-effects models using lme4. *Journal of Statistical Software*, *67*, 1–48. https://doi.org/10.18637/jss.v067.i01

Baxter, I., Hosmani, P. S., Rus, A., Lahner, B., Borevitz, J. O., Muthukumar, B., Mickelbart, M. V., Schreiber, L., Franke, R. B., & Salt, D. E. (2009). Root suberin forms an extracellular barrier that affects water relations and mineral nutrition in arabidopsis. *PLoS Genetics*, *5*(5), e1000492. https://doi.org/10.1371/journal.pgen.1000492

Benjamini, Y., & Hochberg, Y. (1995). Controlling the false discovery rate: A practical and powerful approach to multiple testing. *Journal of the Royal Statistical Society: Series B (Methodological)*, *57*(1), 289–300. https://doi.org/10.1111/j.2517-6161.1995.tb02031.x

Borrell, A. K., Mullet, J. E., George-Jaeggli, B., van Oosterom, E. J., Hammer, G. L., Klein, P. E., & Jordan, D. R. (2014). Drought adaptation of stay-green sorghum is associated with canopy development, leaf anatomy, root growth, and water uptake. *Journal of Experimental Botany*, *65*(21), 6251–6263. https://doi.org/10.1093/jxb/eru232

Bouchet, S., Olatoye, M. O., Marla, S. R., Perumal, R., Tesso, T., Yu, J., Tuinstra, M., & Morris, G. P. (2017). Increased power to dissect adaptive traits in global sorghum diversity using a nested association mapping population. *Genetics*, *206*(2), 573–585. https://doi.org/10.1534/genetics.116.198499

Breitzman, M. W., Bao, Y., Tang, L., Schnable, P. S., & Salas-Fernandez, M. G. (2019). Linkage disequilibrium mapping of high-throughput image-derived descriptors of plant architecture traits under field conditions. *Field Crops Research*, *244*, 107619. https://doi.org/10.1016/j.fcr.2019.107619

Brenton, Z. W., Cooper, E. A., Myers, M. T., Boyles, R. E., Shakoor, N., Zielinski, K. J., Rauh, B. L., Bridges, W. C., Morris, G. P., & Kresovich, S. (2016). A genomic resource for the development, improvement, and exploitation of sorghum for bioenergy. *Genetics*, *204*(1), 21–33. https://doi.org/10.1534/genetics.115.183947

Brown, N. J., Palmer, B. G., Stanley, S., Hajaji, H., Janacek, S. H., Astley, H. M., Parsley, K., Kajala, K., Quick, W. P., Trenkamp, S., Fernie, A. R., Maurino, V. G., & Hibberd, J. M. (2010). C4 acid decarboxylases required for C4 photosynthesis are active in the mid-vein of the C3 species *Arabidopsis thaliana*, and are important in sugar and amino acid metabolism. *The Plant Journal*, *61*(1), 122–133. https://doi.org/10.1111/j.1365-313X.2009.04040.x

Brown, P. J., Rooney, W. L., Franks, C., & Kresovich, S. (2008). Efficient mapping of plant height quantitative Trait Loci in a Sorghum association population with introgressed dwarfing genes. *Genetics*, *180*(1), 629–637. https://doi.org/10.1534/genetics.108.092239

Browning, B. L., & Browning, S. R. (2016). Genotype imputation with millions of reference samples. *The American Journal of Human Genetics*, *98*(1), 116–126. https://doi.org/10.1016/j.ajhg.2015.11.020

Busemeyer, L., Ruckelshausen, A., Möller, K., Melchinger, A. E., Alheit, K. V., Maurer, H. P., Hahn, V., Weissmann, E. A., Reif, J. C., & Würschum, T. (2013). Precision phenotyping of biomass accumulation in triticale reveals temporal genetic patterns of regulation. *Scientific Reports*, *3*(1), 2442. https://doi.org/10.1038/srep02442

Campbell, M. T., Du, Q., Liu, K., Brien, C. J., Berger, B., Zhang, C., & Walia, H. (2017). A comprehensive image-based phenomic analysis reveals the complex genetic architecture of shoot growth dynamics in rice (*Oryza sativa*). *The Plant Genome*, *10*(2), plantgenome2016.07.0064. https://doi.org/10.3835/plantgenome2016.07.0064

Carena, M. J., Hallauer, A. R., & Miranda Filho, J. B. (2010). *Quantitative genetics in maize breeding*. Springer. https://doi.org/10.1007/978-1-4419-0766-0

Casa, A. M., Pressoir, G., Brown, P. J., Mitchell, S. E., Rooney, W. L., Tuinstra, M. R., Franks, C. D., & Kresovich, S. (2008). Community resources and strategies for association mapping in sorghum. *Crop Science*, *48*(1), 30–40. https://doi.org/10.2135/cropsci2007.02.0080

Cass, C. L., Peraldi, A., Dowd, P. F., Mottiar, Y., Santoro, N., Karlen, S. D., Bukhman, Y. V., Foster, C. E., Thrower, N., Bruno, L. C., Moskvin, O. V., Johnson, E. T., Willhoit, M. E., Phutane, M., Ralph, J., Mansfield, S. D., Nicholson, P., & Sedbrook, J. C. (2015). Effects of *PHENYLALANINE AMMONIA LYASE* (*PAL*) knockdown on cell wall composition, biomass digestibility, and biotic and abiotic stress responses in Brachypodium. *Journal of Experimental Botany*, *66*(14), 4317–4335. https://doi.org/10.1093/jxb/erv269

Chateigner-Boutin, A.-L., Suliman, M., Bouchet, B., Alvarado, C., Lollier, V., Rogniaux, H., Guillon, F., & Larré, C. (2015). Endomembrane proteomics reveals putative enzymes involved in cell wall metabolism in wheat grain outer layers. *Journal of Experimental Botany*, *66*(9), 2649–2658. https://doi.org/10.1093/jxb/erv075

Chen, D., Shao, Q., Yin, L., Younis, A., & Zheng, B. (2019). Polyamine function in plants: Metabolism, regulation on development, and roles in abiotic stress responses. *Frontiers in Plant Science*, *9*, 1945. https://www.frontiersin.org/articles/10.3389/fpls.2018.01945

Chen, Y., Cai, Q., & Hao, S. (2017). The maize *brevis plant1* is a type II inositol polyphosphate 5-phosphatase. *Journal of Plant Biochemistry and Biotechnology*, *27*(2), 215–222. https://doi.org/10.1007/s13562-017-0433-7

Curry, T. M., Peña, M. J., & Urbanowicz, B. R. (2023). An update on xylan structure, biosynthesis, and potential commercial applications. *The Cell Surface*, *9*, 100101. https://doi.org/10.1016/j.tcsw.2023.100101

Davin, L. B., & Lewis, N. G. (2000). Dirigent proteins and dirigent sites explain the mystery of specificity of radical precursor coupling in lignan and lignin Biosynthesis1. *Plant Physiology*, *123*(2), 453–462. https://doi.org/10.1104/pp.123.2.453

Day, I. S., Miller, C., Golovkin, M., & Reddy, A. S. N. (2000). Interaction of a kinesin-like calmodulin-binding protein with a protein kinase*. *Journal of Biological Chemistry*, *275*(18), 13737–13745. https://doi.org/10.1074/jbc.275.18.13737

Drincovich, M. F., Casati, P., & Andreo, C. S. (2001). NADP-malic enzyme from plants: A ubiquitous enzyme involved in different metabolic pathways. *FEBS Letters*, *490*(1), 1–6. https://doi.org/10.1016/S0014-5793(00)02331-0

Earl, D. A., & vonHoldt, B. M. (2012). STRUCTURE HARVESTER: A website and program for visualizing STRUCTURE output and implementing the Evanno method. *Conservation Genetics Resources*, *4*(2), 359–361. https://doi.org/10.1007/s12686-011-9548-7

Edwards, G. E., & Andreo, C. S. (1992). NADP-malic enzyme from plants. *Phytochemistry*, *31*(6), 1845–1857. https://doi.org/10.1016/0031-9422(92)80322-6

Felderhoff, T. J., Murray, S. C., Klein, P. E., Sharma, A., Hamblin, M. T., Kresovich, S., Vermerris, W., & Rooney, W. L. (2012). QTLs for energy-related traits in a Sweet × Grain Sorghum [*Sorghum bicolor* (L.) Moench] mapping population. *Crop Science*, *52*(5), 2040–2049. https://doi.org/10.2135/cropsci2011.11.0618

Ferguson, J. N., Fernandes, S. B., Monier, B., Miller, N. D., Allen, D., Dmitrieva, A., Schmuker, P., Lozano, R., Valluru, R., Buckler, E. S., Gore, M. A., Brown, P. J., Spalding, E. P., & Leakey, A. D. B. (2021). Machine learning-enabled phenotyping for GWAS and TWAS of WUE traits in 869 field-grown sorghum accessions. *Plant Physiology*, *187*(3), 1481–1500. https://doi.org/10.1093/plphys/kiab346

Fiedler, K., Bekele, W. A., Duensing, R., Gründig, S., Snowdon, R., Stützel, H., Zacharias, A., & Uptmoor, R. (2014). Genetic dissection of temperature-dependent sorghum growth during juvenile development. *Theoretical and Applied Genetics*, *127*(9), 1935–1948. https://doi.org/10.1007/s00122-014-2350-7

Fornalé, S., Shi, X., Chai, C., Encina, A., Irar, S., Capellades, M., Fuguet, E., Torres, J.-L., Rovira, P., Puigdomènech, P., Rigau, J., Grotewold, E., Gray, J., & Caparrós-Ruiz, D. (2010). ZmMYB31 directly represses maize lignin genes and redirects the phenylpropanoid metabolic flux. *The Plant Journal*, *64*(4), 633–644. https://doi.org/10.1111/j.1365-313X.2010.04363.x

Furbank, R. T., & Tester, M. (2011). Phenomics—Technologies to relieve the phenotyping bottleneck. *Trends in Plant Science*, *16*(12), 635–644. https://doi.org/10.1016/j.tplants.2011.09.005

Gage, J. L., Richards, E., Lepak, N., Kaczmar, N., Soman, C., Chowdhary, G., Gore, M. A., & Buckler, E. S. (2019). In-field whole-plant maize architecture characterized by subcanopy rovers and latent space phenotyping. *The Plant Phenome Journal*, *2*(1), 190011. https://doi.org/10.2135/tppj2019.07.0011

Gaillard, M., Miao, C., Schnable, J. C., & Benes, B. (2020). Voxel carving-based 3D reconstruction of sorghum identifies genetic determinants of light interception efficiency. *Plant Direct*, *4*(10), e00255. https://doi.org/10.1002/pld3.255

George-Jaeggli, B., Mortlock, M. Y., & Borrell, A. K. (2017). Bigger is not always better: Reducing leaf area helps stay-green sorghum use soil water more slowly. *Environmental and Experimental Botany*, *138*, 119–129. https://doi.org/10.1016/j.envexpbot.2017.03.002

Goldsworthy, P. R. (1970). The canopy structure of tall and short sorghum. *The Journal of Agricultural Science*, *75*(1), 123–131. https://doi.org/10.1017/S0021859600026125

Hartmann, J., Fischer, C., Dietrich, P., & Sauter, M. (2014). Kinase activity and calmodulin binding are essential for growth signaling by the phytosulfokine receptor PSKR1. *The Plant Journal*, *78*(2), 192–202. https://doi.org/10.1111/tpj.12460

Haussmann, B., Mahalakshmi, V., Reddy, B., Seetharama, N., Hash, C., & Geiger, H. (2002). QTL mapping of stay-green in two sorghum recombinant inbred populations. *Theoretical and Applied Genetics*, *106*(1), 133–142. https://doi.org/10.1007/s00122-002-1012-3

Hepler, P. K. (2005). Calcium: A central regulator of plant growth and development. *The Plant Cell*, *17*(8), 2142–2155. https://doi.org/10.1105/tpc.105.032508

Higgins, R. H., Thurber, C. S., Assaranurak, I., & Brown, P. J. (2014). Multiparental mapping of plant height and flowering time QTL in partially isogenic sorghum families. *G3 Genes|Genomes|Genetics*, *4*(9), 1593–1602. https://doi.org/10.1534/g3.114.013318

Hilley, J., Truong, S., Olson, S., Morishige, D., & Mullet, J. (2016). Identification of *Dw1*, a regulator of sorghum stem internode length. *PLoS One*, *11*(3), e0151271. https://doi.org/10.1371/journal.pone.0151271

Hilley, J. L., Weers, B. D., Truong, S. K., McCormick, R. F., Mattison, A. J., McKinley, B. A., Morishige, D. T., & Mullet, J. E. (2017). Sorghum *Dw2* encodes a protein kinase regulator of stem internode length. *Scientific Reports*, *7*(1), 4616. https://doi.org/10.1038/s41598-017-04609-5

Hosmani, P. S., Kamiya, T., Danku, J., Naseer, S., Geldner, N., Guerinot, M. L., & Salt, D. E. (2013). Dirigent domain-containing protein is part of the machinery required for formation of the lignin-based Casparian strip in the root. *Proceedings of the National Academy of Sciences*, *110*(35), 14498–14503. https://doi.org/10.1073/pnas.1308412110

Hu, P., Chapman, S. C., Wang, X., Potgieter, A., Duan, T., Jordan, D., Guo, Y., & Zheng, B. (2018). Estimation of plant height using a high throughput phenotyping platform based on unmanned aerial vehicle and self-calibration: Example for sorghum breeding. *European Journal of Agronomy*, *95*, 24–32. https://doi.org/10.1016/j.eja.2018.02.004

Humphrey, T. V., Haasen, K. E., Aldea-Brydges, M. G., Sun, H., Zayed, Y., Indriolo, E., & Goring, D. R. (2015). PERK–KIPK–KCBP signalling negatively regulates root growth in *Arabidopsis thaliana*. *Journal of Experimental Botany*, *66*(1), 71–83. https://doi.org/10.1093/jxb/eru390

Jaikumar, N. S., Stutz, S. S., Fernandes, S. B., Leakey, A. D., Bernacchi, C. J., Brown, P. J., & Long, S. P. (2021). Can improved canopy light transmission ameliorate loss of photosynthetic efficiency in the shade? An investigation of natural variation in Sorghum bicolor. *Journal of Experimental Botany*, *72*(13), 4965–4980.

Jiang, Y., Li, C., Robertson, J. S., Sun, S., Xu, R., & Paterson, A. H. (2018). GPhenoVision: A ground mobile system with multi-modal imaging for field-based high throughput phenotyping of cotton. *Scientific Reports*, *8*(1), 1213. https://doi.org/10.1038/s41598-018-19142-2

Joshi, D. C., Singh, V., Hunt, C., Mace, E., van Oosterom, E., Sulman, R., Jordan, D., & Hammer, G. (2017). Development of a phenotyping platform for high throughput screening of nodal root angle in sorghum. *Plant Methods*, *13*(1), 56. https://doi.org/10.1186/s13007-017-0206-2

Jun, S.-Y., Sattler, S. A., Cortez, G. S., Vermerris, W., Sattler, S. E., & Kang, C. (2018). Biochemical and structural analysis of substrate specificity of a phenylalanine ammonia-lyase. *Plant Physiology*, *176*(2), 1452–1468. https://doi.org/10.1104/pp.17.01608

Kapanigowda, M. H., Payne, W. A., Rooney, W. L., Mullet, J. E., & Balota, M. (2014). Quantitative trait locus mapping of the transpiration ratio related to preflowering drought tolerance in sorghum (*Sorghum bicolor*). *Functional Plant Biology: FPB*, *41*(11), 1049–1065. https://doi.org/10.1071/FP13363

Kim, H. K., van Oosterom, E., Dingkuhn, M., Luquet, D., & Hammer, G. (2010). Regulation of tillering in sorghum: Environmental effects. *Annals of Botany*, *106*(1), 57–67. https://doi.org/10.1093/aob/mcq079

Kouressy, M., Dingkuhn, M., Vaksmann, M., Clément-Vidal, A., & Chantereau, J. (2008). Potential contribution of dwarf and leaf longevity traits to yield improvement in photoperiod sensitive sorghum. *European Journal of Agronomy*, *28*(3), 195–209. https://doi.org/10.1016/j.eja.2007.07.008

Lafarge, T. A., Broad, I. J., & Hammer, G. L. (2002). Tillering in grain sorghum over a wide range of population densities: Identification of a common hierarchy for tiller emergence, leaf area development and fertility. *Annals of Botany*, *90*(1), 87–98. https://doi.org/10.1093/aob/mcf152

Lafarge, T. A., & Hammer, G. L. (2002). Tillering in grain sorghum over a wide range of population densities: Modelling dynamics of tiller fertility. *Annals of Botany*, *90*(1), 99–110. https://doi.org/10.1093/aob/mcf153

Lee, C., Zhong, R., & Ye, Z.-H. (2012). Arabidopsis family GT43 members are Xylan Xylosyltransferases required for the Elongation of the Xylan backbone. *Plant and Cell Physiology*, *53*(1), 135–143. https://doi.org/10.1093/pcp/pcr158

Lenth, R. V., Bolker, B., Buerkner, P., Giné-Vázquez, I., Herve, M., Jung, M., Love, J., Miguez, F., Riebl, H., & Singmann, H. (2023). *emmeans: Estimated marginal means, aka least-squares means* (1.8.8) [Computer software]. https://cran.r-project.org/web/packages/emmeans/index.html

Li, L., Yu, X., Zhang, S., Zhao, X., & Zhang, L. (2017). 3D cost aggregation with multiple minimum spanning trees for stereo matching. *Applied Optics*, *56*(12), 3411–3420. https://doi.org/10.1364/AO.56.003411

Li, Z., Wang, X., Yang, K., Zhu, C., Yuan, T., Wang, J., Li, Y., & Gao, Z. (2021). Identification and expression analysis of the glycosyltransferase GT43 family members in bamboo reveal their potential function in xylan biosynthesis during rapid growth. *BMC Genomics*, *22*(1), 867. https://doi.org/10.1186/s12864-021-08192-y

Liu, F., Song, Q., Zhao, J., Mao, L., Bu, H., Hu, Y., & Zhu, X.-G. (2021). Canopy occupation volume as an indicator of canopy photosynthetic capacity. *New Phytologist*, *232*(2), 941–956. https://doi.org/10.1111/nph.17611

Liu, X., Huang, M., Fan, B., Buckler, E. S., & Zhang, Z. (2016). Iterative usage of fixed and random effect models for powerful and efficient genome-wide association studies. *PLoS Genetics*, *12*(2), e1005767. https://doi.org/10.1371/journal.pgen.1005767

Long, S. P., Zhu, X.-G., Naidu, S. L., & Ort, D. R. (2006). Can improvement in photosynthesis increase crop yields? *Plant, Cell & Environment*, *29*(3), 315–330. https://doi.org/10.1111/j.1365-3040.2005.01493.x

Lovegrove, A., Wilkinson, M. D., Freeman, J., Pellny, T. K., Tosi, P., Saulnier, L., Shewry, P. R., & Mitchell, R. A. C. (2013). RNA interference suppression of genes in Glycosyl transferase families 43 and 47 in wheat starchy endosperm causes large decreases in arabinoxylan content. *Plant Physiology*, *163*(1), 95–107. https://doi.org/10.1104/pp.113.222653

Lyra, D. H., Virlet, N., Sadeghi-Tehran, P., Hassall, K. L., Wingen, L. U., Orford, S., Griffiths, S., Hawkesford, M. J., & Slavov, G. T. (2020). Functional QTL mapping and genomic prediction of canopy height in wheat measured using a robotic field phenotyping platform. *Journal of Experimental Botany*, *71*(6), 1885–1898. https://doi.org/10.1093/jxb/erz545

Mace, E. S., Innes, D., Hunt, C., Wang, X., Tao, Y., Baxter, J., Hassall, M., Hathorn, A., & Jordan, D. (2019). The Sorghum QTL Atlas: A powerful tool for trait dissection, comparative genomics and crop improvement. *Theoretical and Applied Genetics*, *132*(3), 751–766. https://doi.org/10.1007/s00122-018-3212-5

Mace, E. S., Singh, V., van Oosterom, E. J., Hammer, G. L., Hunt, C. H., & Jordan, D. R. (2012). QTL for nodal root angle in sorghum (*Sorghum bicolor* L. Moench) co-locate with QTL for traits associated with drought adaptation. *Theoretical and Applied Genetics*, *124*(1), 97–109. https://doi.org/10.1007/s00122-011-1690-9

Mantilla-Perez, M. B., Bao, Y., Tang, L., Schnable, P. S., & Salas-Fernandez, M. G. (2020). Toward "smart canopy" sorghum: Discovery of the genetic control of leaf angle across layers. *Plant Physiology*, *184*(4), 1927–1940.

Mantilla-Perez, M. B., & Salas Fernandez, M. G. (2017). Differential manipulation of leaf angle throughout the canopy: Current status and prospects. *Journal of Experimental Botany*, *68*(21–22), 5699–5717. https://doi.org/10.1093/jxb/erx378

Mantilla Perez, M. B., Zhao, J., Yin, Y., Hu, J., & Salas Fernandez, M. G. (2014). Association mapping of brassinosteroid candidate genes and plant architecture in a diverse panel of Sorghum bicolor. *Theoretical and Applied Genetics*, *127*(12), 2645–2662. https://doi.org/10.1007/s00122-014-2405-9

McCormick, R. F., Truong, S. K., & Mullet, J. E. (2016). 3D sorghum reconstructions from depth images identify QTL regulating shoot Architecture. *Plant Physiology*, *172*(2), 823–834. https://doi.org/10.1104/pp.16.00948

Miao, C., Pages, A., Xu, Z., Rodene, E., Yang, J., & Schnable, J. C. (2020). Semantic segmentation of sorghum using hyperspectral data identifies genetic associations. *Plant Phenomics*, *2020*, 4216373. https://doi.org/10.34133/2020/4216373

Miao, C., Xu, Y., Liu, S., Schnable, P. S., & Schnable, J. C. (2020). Increased power and accuracy of causal locus identification in time series genome-wide association in Sorghum. *Plant Physiology*, *183*(4), 1898–1909. https://doi.org/10.1104/pp.20.00277

Mocoeur, A., Zhang, Y.-M., Liu, Z.-Q., Shen, X., Zhang, L.-M., Rasmussen, S. K., & Jing, H.-C. (2015). Stability and genetic control of morphological, biomass and biofuel traits under temperate maritime and continental conditions in sweet sorghum (*Sorghum bicolour*). *Theoretical and Applied Genetics*, *128*(9), 1685–1701. https://doi.org/10.1007/s00122-015-2538-5

Morris, G. P., Ramu, P., Deshpande, S. P., Hash, C. T., Shah, T., Upadhyaya, H. D., Riera-Lizarazu, O., Brown, P. J., Acharya, C. B., Mitchell, S. E., Harriman, J., Glaubitz, J. C., Buckler, E. S., & Kresovich, S. (2013). Population genomic and genome-wide association studies of agroclimatic traits in sorghum. *Proceedings of the National Academy of Sciences*, *110*(2), 453–458. https://doi.org/10.1073/pnas.1215985110

Mu, Q., Guo, T., Li, X., & Yu, J. (2022). Phenotypic plasticity in plant height shaped by interaction between genetic loci and diurnal temperature range. *New Phytologist*, *233*(4), 1768–1779. https://doi.org/10.1111/nph.17904

Muraya, M. M., Chu, J., Zhao, Y., Junker, A., Klukas, C., Reif, J. C., & Altmann, T. (2017). Genetic variation of growth dynamics in maize (*Zea mays* L.) revealed through automated non-invasive phenotyping. *The Plant Journal*, *89*(2), 366–380. https://doi.org/10.1111/tpj.13390

Multani, D. S., Briggs, S. P., Chamberlin, M. A., Blakeslee, J. J., Murphy, A. S., & Johal, G. S. (2003). Loss of an MDR transporter in compact stalks of maize br2 and sorghum dw3 mutants. *Science*, *302*(5642), 81–84. https://doi.org/10.1126/science.1086072

Murray, S. C., Rooney, W. L., Hamblin, M. T., Mitchell, S. E., & Kresovich, S. (2009). Sweet sorghum genetic diversity and association mapping for brix and height. *The Plant Genome*, *2*(1). https://doi.org/10.3835/plantgenome2008.10.0011

Nagaraja Reddy, R., Madhusudhana, R., Murali Mohan, S., Chakravarthi, D. V. N., Mehtre, S. P., Seetharama, N., & Patil, J. V. (2013). Mapping QTL for grain yield and other agronomic traits in post-rainy sorghum [*Sorghum bicolor* (L.) Moench]. *Theoretical and Applied Genetics*, *126*(8), 1921–1939. https://doi.org/10.1007/s00122-013-2107-8

Natukunda, M. I., Mantilla-Perez, M. B., Graham, M. A., Liu, P., & Salas-Fernandez, M. G. (2022). Dissection of canopy layer-specific genetic control of leaf angle in Sorghum bicolor by RNA sequencing. *BMC Genomics*, *23*(1), 95. https://doi.org/10.1186/s12864-021-08251-4

Neilson, E. H., Edwards, A. M., Blomstedt, C. K., Berger, B., Møller, B. L., & Gleadow, R. M. (2015). Utilization of a high-throughput shoot imaging system to examine the dynamic phenotypic responses of a C4 cereal crop plant to nitrogen and water deficiency over time. *Journal of Experimental Botany*, *66*(7), 1817–1832. https://doi.org/10.1093/jxb/eru526

Ngara, R., Ramulifho, E., Movahedi, M., Shargie, N. G., Brown, A. P., & Chivasa, S. (2018). Identifying differentially expressed proteins in sorghum cell cultures exposed to osmotic stress. *Scientific Reports*, *8*, 8671. https://doi.org/10.1038/s41598-018-27003-1

Nielsen, L. J., Stuart, P., Pičmanová, M., Rasmussen, S., Olsen, C. E., Harholt, J., Møller, B. L., & Bjarnholt, N. (2016). Dhurrin metabolism in the developing grain of *Sorghum bicolor* (L.) Moench investigated by metabolite profiling and novel clustering analyses of time-resolved transcriptomic data. *BMC Genomics*, *17*(1), 1021. https://doi.org/10.1186/s12864-016-3360-4

Olatoye, M. O., Hu, Z., & Morris, G. P. (2020). Genome-wide mapping and prediction of plant architecture in a sorghum nested association mapping population. *The Plant Genome*, *13*(3), e20038.

Olson, S. N., Ritter, K., Rooney, W., Kemanian, A., McCarl, B. A., Zhang, Y., Hall, S., Packer, D., & Mullet, J. (2012). High biomass yield energy sorghum: Developing a genetic model for C4 grass bioenergy crops. *Biofuels, Bioproducts and Biorefining*, *6*(6), 640–655. https://doi.org/10.1002/bbb.1357

Ort, D. R., Merchant, S. S., Alric, J., Barkan, A., Blankenship, R. E., Bock, R., Croce, R., Hanson, M. R., Hibberd, J. M., Long, S. P., Moore, T. A., Moroney, J., Niyogi, K. K., Parry, M. A. J., Peralta-Yahya, P. P., Prince, R. C., Redding, K. E., Spalding, M. H., van Wijk, K. J., … Zhu, X. G. (2015). Redesigning photosynthesis to sustainably meet global food and bioenergy demand. *Proceedings of the National Academy of Sciences*, *112*(28), 8529–8536. https://doi.org/10.1073/pnas.1424031112

Ott, A., Liu, S., Schnable, J. C., Yeh, C. T. E., Wang, K. S., & Schnable, P. S. (2017). tGBS® genotyping-by-sequencing enables reliable genotyping of heterozygous loci. *Nucleic Acids Research*, *45*(21), e178.

Paniagua, C., Bilkova, A., Jackson, P., Dabravolski, S., Riber, W., Didi, V., Houser, J., Gigli-Bisceglia, N., Wimmerova, M., Budínská, E., Hamann, T., & Hejatko, J. (2017). Dirigent proteins in plants: Modulating cell wall metabolism during abiotic and biotic stress exposure. *Journal of Experimental Botany*, *68*(13), 3287–3301. https://doi.org/10.1093/jxb/erx141

Paterson, A. H., Schertz, K. F., Lin, Y. R., Liu, S. C., & Chang, Y. L. (1995). The weediness of wild plants: Molecular analysis of genes influencing dispersal and persistence of johnsongrass, *Sorghum halepense* (L.) Pers. *Proceedings of the National Academy of Sciences*, *92*(13), 6127–6131. https://doi.org/10.1073/pnas.92.13.6127

Perez, R. P. A., Fournier, C., Cabrera-Bosquet, L., Artzet, S., Pradal, C., Brichet, N., Chen, T.-W., Chapuis, R., Welcker, C., & Tardieu, F. (2019). Changes in the vertical distribution of leaf area enhanced light interception efficiency in maize over generations of selection. *Plant, Cell & Environment*, *42*(7), 2105–2119. https://doi.org/10.1111/pce.13539

Perrier, L., Rouan, L., Jaffuel, S., Clément-Vidal, A., Roques, S., Soutiras, A., Baptiste, C., Bastianelli, D., Fabre, D., Dubois, C., Pot, D., & Luquet, D. (2017). Plasticity of sorghum stem biomass accumulation in response to water deficit: A multiscale analysis from internode tissue to plant level. *Frontiers in Plant Science*, *8*, 1516. https://www.frontiersin.org/articles/10.3389/fpls.2017.01516

Pfeiffer, B. K., Pietsch, D., Schnell, R. W., & Rooney, W. L. (2019). Long-term selection in hybrid sorghum breeding programs. *Crop Science*, *59*(1), 150–164. https://doi.org/10.2135/cropsci2018.05.0345

Phuong, N., Stützel, H., & Uptmoor, R. (2013). Quantitative trait loci associated to agronomic traits and yield components in a *Sorghum bicolor* L. Moench RIL population cultivated under pre-flowering drought and well-watered conditions. *Agricultural Sciences*, *4*(12), 781–791. https://doi.org/10.15488/1536

Piotrowski, M., Janowitz, T., & Kneifel, H. (2003). Plant C-N hydrolases and the identification of a plant N-carbamoylputrescine amidohydrolase involved in polyamine biosynthesis. *The Journal of Biological Chemistry*, *278*(3), 1708–1712. https://doi.org/10.1074/jbc.M205699200

Poorter, H., Fiorani, F., Pieruschka, R., Wojciechowski, T., van der Putten, W. H., Kleyer, M., Schurr, U., & Postma, J. (2016). Pampered inside, pestered outside? Differences and similarities between plants growing in controlled conditions and in the field. *New Phytologist*, *212*(4), 838–855. https://doi.org/10.1111/nph.14243

Price, M. N., & Arkin, A. P. (2017). PaperBLAST: Text mining papers for information about homologs. *mSystems*, *2*(4), e00039–e00017. https://doi.org/10.1128/mSystems.00039-17

Pritchard, J. K., Stephens, M., & Donnelly, P. (2000). Inference of population structure using multilocus genotype data. *Genetics*, *155*(2), 945–959. https://doi.org/10.1093/genetics/155.2.945

Pugh, N. A., Horne, D. W., Murray, S. C., Carvalho, G. Jr., Malambo, L., Jung, J., Chang, A., Maeda, M., Popescu, S., Chu, T., Starek, M. J., Brewer, M. J., Richardson, G., & Rooney, W. L. (2018). Temporal estimates of crop growth in sorghum and maize breeding enabled by unmanned aerial systems. *The Plant Phenome Journal*, *1*(1), 170006. https://doi.org/10.2135/tppj2017.08.0006

Qiang, Z., Sun, H., Ge, F., Li, W., Li, C., Wang, S., Zhang, B., Zhu, L., Zhang, S., Wang, X., Lai, J., Qin, F., Zhou, Y., & Fu, Y. (2022). The transcription factor ZmMYB69 represses lignin biosynthesis by activating ZmMYB31/42 expression in maize. *Plant Physiology*, *189*(4), 1916–1919. https://doi.org/10.1093/plphys/kiac233

Quinby, J. R., & Karper, R. E. (1953). Inheritance of height in sorghum. *Inheritance of Height in Sorghum*, *46*(5), 211–216. https://www.cabdirect.org/cabdirect/abstract/19541603750

R Core Team. (2023). *R: A language and environment for statistial computing*. R Foundation for Statistical Computing. https://www.R-project.org/

Rodrigues Castro, F. M., Lombardi, G. M. R., Nunes, J. A. R., Parrella, R. A. d. C., & Bruzi, A. T. (2022). Accumulation of biomass and lignocellulosic compounds in photoperiod-sensitive biomass sorghum genotypes. *Biomass and Bioenergy*, *158*, 106344. https://doi.org/10.1016/j.biombioe.2022.106344

Rosler, J., Krekel, F., Amrhein, N., & Schmid, J. (1997). Maize phenylalanine ammonia-lyase has tyrosine ammonia-lyase activity. *Plant Physiology*, *113*(1), 175–179. https://doi.org/10.1104/pp.113.1.175

Salas Fernandez, M. G., Bao, Y., Tang, L., & Schnable, P. S. (2017). A high-throughput, field-based phenotyping technology for tall biomass crops. *Plant Physiology*, *174*(4), 2008–2022. https://doi.org/10.1104/pp.17.00707

Salas-Fernandez, M. G., Becraft, P. W., Yin, Y., & Lübberstedt, T. (2009). From dwarves to giants? Plant height manipulation for biomass yield. *Trends in Plant Science*, *14*(8), 454–461. https://doi.org/10.1016/j.tplants.2009.06.005

Salas-Fernandez, M. G., & Kemp, J. (2022). Registration of IA100RPS and IA101RPS sorghum inbred lines for photoperiod-sensitive biomass hybrids. *Journal of Plant Registrations*, *16*(2), 465–472. https://doi.org/10.1002/plr2.20199

Sato-Izawa, K., Nakaba, S., Tamura, K., Yamagishi, Y., Nakano, Y., Nishikubo, N., Kawai, S., Kajita, S., Ashikari, M., Funada, R., Katayama, Y., & Kitano, H. (2012). DWARF50 (D50), a rice (*Oryza sativa* L.) gene encoding inositol polyphosphate 5-phosphatase, is required for proper development of intercalary meristem. *Plant, Cell & Environment*, *35*(11), 2031–2044. https://doi.org/10.1111/j.1365-3040.2012.02534.x

Scheller, H. V., & Ulvskov, P. (2010). Hemicelluloses. *Annual Review of Plant Biology*, *61*, 263–289. https://doi.org/10.1146/annurev-arplant-042809-112315

Sekula, B., Ruszkowski, M., Malinska, M., & Dauter, Z. (2016). Structural investigations of n-carbamoylputrescine amidohydrolase from medicago truncatula: Insights into the ultimate step of putrescine biosynthesis in plants. *Frontiers in Plant Science*, *7*, 350. https://www.frontiersin.org/articles/10.3389/fpls.2016.00350

Shiringani, A. L., Frisch, M., & Friedt, W. (2010). Genetic mapping of QTLs for sugar-related traits in a RIL population of *Sorghum bicolor* L. Moench. *Theoretical and Applied Genetics*, *121*(2), 323–336. https://doi.org/10.1007/s00122-010-1312-y

Sonbol, F.-M., Fornalé, S., Capellades, M., Encina, A., Touriño, S., Torres, J.-L., Rovira, P., Ruel, K., Puigdomènech, P., Rigau, J., & Caparrós-Ruiz, D. (2009). The maize ZmMYB42 represses the phenylpropanoid pathway and affects the cell wall structure, composition and degradability in Arabidopsis thaliana. *Plant Molecular Biology*, *70*(3), 283–296. https://doi.org/10.1007/s11103-009-9473-2

Song, Q., Zhang, G., & Zhu, X.-G. (2013). Optimal crop canopy architecture to maximise canopy photosynthetic $CO_2$ uptake under elevated CO2—A theoretical study using a mechanistic model of canopy photosynthesis. *Functional Plant Biology*, *40*(2), 108. https://doi.org/10.1071/FP12056

Spindel, J. E., Dahlberg, J., Colgan, M., Hollingsworth, J., Sievert, J., Staggenborg, S. H., Hutmacher, R., Jansson, C., & Vogel, J. P. (2018). Association mapping by aerial drone reveals 213 genetic associations for *Sorghum bicolor* biomass traits under drought. *BMC Genomics*, *19*(1), 679. https://doi.org/10.1186/s12864-018-5055-5

Sun, S., Li, C., Paterson, A. H., Jiang, Y., Xu, R., Robertson, J. S., Snider, J. L., & Chee, P. W. (2018). In-field high throughput phenotyping and cotton plant growth analysis using LiDAR. *Frontiers in Plant Science*, *9*, 16. https://www.frontiersin.org/articles/10.3389/fpls.2018.00016

Takenawa, T., & Itoh, T. (2001). Phosphoinositides, key molecules for regulation of actin cytoskeletal organization and membrane traffic from the plasma membrane. *Biochimica et Biophysica Acta (BBA)—Molecular and Cell Biology of Lipids*, *1533*(3), 190–206. https://doi.org/10.1016/S1388-1981(01)00165-2

Tanger, P., Klassen, S., Mojica, J. P., Lovell, J. T., Moyers, B. T., Baraoidan, M., Naredo, M. E. B., McNally, K. L., Poland, J., Bush, D. R., Leung, H., Leach, J. E., & McKay, J. K. (2017). Field-based high throughput phenotyping rapidly identifies genomic regions controlling yield components in rice. *Scientific Reports*, *7*(1), 42839. https://doi.org/10.1038/srep42839

Teh, C. B. S., Simmonds, L. P., & Wheeler, T. R. (2000). An equation for irregular distributions of leaf azimuth density. *Agricultural and Forest Meteorology*, *102*(4), 223–234. https://doi.org/10.1016/S0168-1923(00)00132-5

Truong, S. K., McCormick, R. F., Rooney, W. L., & Mullet, J. E. (2015). Harnessing genetic variation in leaf angle to increase productivity of Sorghum bicolor. *Genetics*, *201*(3), 1229–1238.

Varela, S., Pederson, T., Bernacchi, C. J., & Leakey, A. D. B. (2021). Understanding growth dynamics and yield prediction of sorghum using high temporal resolution UAV imagery time series and machine learning. *Remote Sensing*, *13*(9), 1763. https://doi.org/10.3390/rs13091763

Vijayarangan, S., Sodhi, P., Kini, P., Bourne, J., Du, S., Sun, H., Poczos, B., Apostolopoulos, D., & Wettergreen, D. (2018). High-throughput robotic phenotyping of energy sorghum crops. In M. Hutter & R. Siegwart (Eds.), *Field and service robotics* (pp. 99–113). Springer International Publishing. https://doi.org/10.1007/978-3-319-67361-5_7

Wang, J., & Zhang, Z. (2021). GAPIT version 3: Boosting power and accuracy for genomic association and prediction. *Genomics, Proteomics & Bioinformatics*, *19*(4), 629–640. https://doi.org/10.1016/j.gpb.2021.08.005

Wang, L., Liu, Y., Gao, L., Yang, X., Zhang, X., Xie, S., Chen, M., Wang, Y.-H., Li, J., & Shen, Y. (2022). Identification of candidate forage yield genes in Sorghum (*Sorghum bicolor* L.) using integrated genome-wide association studies and RNA-Seq. *Frontiers in Plant Science*, *12*, 788433. https://www.frontiersin.org/articles/10.3389/fpls.2021.788433

Wang, L., Liu, Z., Han, S., Liu, P., Sadeghnezhad, E., & Liu, M. (2023). Growth or survival: What is the role of calmodulin-like proteins in plant? *International Journal of Biological Macromolecules*, *242*, 124733. https://doi.org/10.1016/j.ijbiomac.2023.124733

Wang, W., Guo, W., Le, L., Yu, J., Wu, Y., Li, D., Wang, Y., Wang, H., Lu, X., Qiao, H., Gu, X., Tian, J., Zhang, C., & Pu, L. (2023). Integration of high-throughput phenotyping, GWAS, and predictive models reveals the genetic architecture of plant height in maize. *Molecular Plant*, *16*(2), 354–373. https://doi.org/10.1016/j.molp.2022.11.016

Ward, B., Brien, C., Oakey, H., Pearson, A., Negrão, S., Schilling, R. K., Taylor, J., Jarvis, D., Timmins, A., Roy, S. J., Tester, M., Berger, B., & van den Hengel, A. (2019). High-throughput 3D modelling to dissect the genetic control of leaf elongation in barley (*Hordeum vulgare*). *The Plant Journal*, *98*(3), 555–570. https://doi.org/10.1111/tpj.14225

Watanabe, K., Guo, W., Arai, K., Takanashi, H., Kajiya-Kanegae, H., Kobayashi, M., Yano, K., Tokunaga, T., Fujiwara, T., Tsutsumi, N., & Iwata, H. (2017). High-throughput phenotyping of sorghum plant height using an unmanned aerial vehicle and its application to genomic prediction modeling. *Frontiers in Plant Science*, *8*, 421. https://www.frontiersin.org/articles/10.3389/fpls.2017.00421

Wei, T., & Simko, V. (2021). *R package 'corrplot': Visualization of a correlation matrix* (Version 0.92). https://github.com/taiyun/corrplot

Weiss, M., Baret, F., Smith, G. J., Jonckheere, I., & Coppin, P. (2004). Review of methods for in situ leaf area index (LAI) determination: Part II. Estimation of LAI, errors and sampling. *Agricultural and Forest Meteorology*, *121*(1), 37–53. https://doi.org/10.1016/j.agrformet.2003.08.001

Whisstock, J. C., Wiradjaja, F., Waters, J. E., & Gurung, R. (2002). The structure and function of catalytic domains within inositol polyphosphate 5-phosphatases. *IUBMB Life (International Union of*

*Biochemistry and Molecular Biology: Life)*, *53*(1), 15–23. https://doi.org/10.1080/15216540210814

Whitehead, C., Ostos Garrido, F. J., Reymond, M., Simister, R., Distelfeld, A., Atienza, S. G., Piston, F., Gomez, L. D., & McQueen-Mason, S. J. (2018). A glycosyl transferase family 43 protein involved in xylan biosynthesis is associated with straw digestibility in *Brachypodium distachyon*. *New Phytologist*, *218*(3), 974–985. https://doi.org/10.1111/nph.15089

Wickham, H., Averick, M., Bryan, J., Chang, W., McGowan, L. D., François, R., Grolemund, G., Hayes, A., Henry, L., Hester, J., Kuhn, M., Pedersen, T. L., Miller, E., Bache, S. M., Müller, K., Ooms, J., Robinson, D., Seidel, D. P., Spinu, V., … Yutani, H. (2019). Welcome to the tidyverse. *Journal of Open Source Software*, *4*(43), 1686. https://doi.org/10.21105/joss.01686

Witt Hmon, K. P., Shehzad, T., & Okuno, K. (2014). QTLs underlying inflorescence architecture in sorghum (*Sorghum bicolor* (L.) Moench) as detected by association analysis. *Genetic Resources and Crop Evolution*, *61*(8), 1545–1564. https://doi.org/10.1007/s10722-014-0129-y

Wu, A.-M., Hörnblad, E., Voxeur, A., Gerber, L., Rihouey, C., Lerouge, P., & Marchant, A. (2010). Analysis of the arabidopsis IRX9/IRX9-L and IRX14/IRX14-L pairs of glycosyltransferase genes reveals critical contributions to biosynthesis of the hemicellulose glucuronoxylan. *Plant Physiology*, *153*(2), 542–554. https://doi.org/10.1104/pp.110.154971

Xu, R., & Li, C. (2022). A review of high-throughput field phenotyping systems: Focusing on ground robots. *Plant Phenomics*, *2022*, 2022/9760269. https://doi.org/10.34133/2022/9760269

Yamaguchi, M., Fujimoto, H., Hirano, K., Araki-Nakamura, S., Ohmae-Shinohara, K., Fujii, A., Tsunashima, M., Song, X. J., Ito, Y., Nagae, R., Wu, J., Mizuno, H., Yonemaru, J., Matsumoto, T., Kitano, H., Matsuoka, M., Kasuga, S., & Sazuka, T. (2016). Sorghum *Dw1*, an agronomically important gene for lodging resistance, encodes a novel protein involved in cell proliferation. *Scientific Reports*, *6*(1), 28366. https://doi.org/10.1038/srep28366

Young, S. N., Kayacan, E., & Peschel, J. M. (2019). Design and field evaluation of a ground robot for high-throughput phenotyping of energy sorghum. *Precision Agriculture*, *20*(4), 697–722. https://doi.org/10.1007/s11119-018-9601-6

Yu, X., Li, X., Guo, T., Zhu, C., Wu, Y., Mitchell, S. E., Roozeboom, K. L., Wang, D., Wang, M. L., Pederson, G. A., Tesso, T. T., Schnable, P. S., Bernardo, R., & Yu, J. (2016). Genomic prediction contributing to a promising global strategy to turbocharge gene banks. *Nature Plants*, *2*(10), 10. https://doi.org/10.1038/nplants.2016.150

Zeng, W., Lampugnani, E. R., Picard, K. L., Song, L., Wu, A.-M., Farion, I. M., Zhao, J., Ford, K., Doblin, M. S., & Bacic, A. (2016). Asparagus IRX9, IRX10, and IRX14A are components of an active Xylan backbone synthase complex that forms in the golgi apparatus. *Plant Physiology*, *171*(1), 93–109. https://doi.org/10.1104/pp.15.01919

Zhang, X., & Liu, C.-J. (2015). Multifaceted regulations of gateway enzyme phenylalanine ammonia-lyase in the biosynthesis of phenylpropanoids. *Molecular Plant*, *8*(1), 17–27. https://doi.org/10.1016/j.molp.2014.11.001

Zhao, J., Mantilla Perez, M. B., Hu, J., & Salas Fernandez, M. G. (2016). Genome-wide association study for nine plant architecture traits in Sorghum. *The Plant Genome*, *9*(2). https://doi.org/10.3835/plantgenome2015.06.0044

Zhi, X., Massey-Reed, S. R., Wu, A., Potgieter, A., Borrell, A., Hunt, C., Jordan, D., Zhao, Y., Chapman, S., Hammer, G., & George-Jaeggli, B. (2022). Estimating photosynthetic attributes from high-throughput canopy hyperspectral sensing in sorghum. *Plant Phenomics*, *2022*, 2022/9768502. https://doi.org/10.34133/2022/9768502

Zhi, X., Tao, Y., Jordan, D., Borrell, A., Hunt, C., Cruickshank, A., Potgieter, A., Wu, A., Hammer, G., & George-Jaeggli, B. (2022). Genetic control of leaf angle in sorghum and its effect on light interception. *Journal of Experimental Botany*, *73*(3), 801–816.

Zhong, R., Burk, D. H., Morrison, W. H., III, & Ye, Z.-H. (2004). *FRAGILE FIBER3*, an arabidopsis gene encoding a type II inositol polyphosphate 5-phosphatase, is required for secondary wall synthesis and actin organization in fiber cells. *The Plant Cell*, *16*(12), 3242–3259. https://doi.org/10.1105/tpc.104.027466

Zou, G., Zhai, G., Feng, Q., Yan, S., Wang, A., Zhao, Q., Shao, J., Zhang, Z., Zou, J., Han, B., & Tao, Y. (2012). Identification of QTLs for eight agronomically important traits using an ultra-high-density map based on SNPs generated from high-throughput sequencing in sorghum under contrasting photoperiods. *Journal of Experimental Botany*, *63*(15), 5451–5462. https://doi.org/10.1093/jxb/ers205

## SUPPORTING INFORMATION

Additional supporting information can be found online in the Supporting Information section at the end of this article.

**How to cite this article:** Panelo, J. S., Bao, Y., Tang, L., Schnable, P. S., & Salas-Fernandez, M. G. (2024). Genetics of canopy architecture dynamics in photoperiod-sensitive and photoperiod-insensitive sorghum. *The Plant Phenome Journal*, *7,* e20092. https://doi.org/10.1002/ppj2.20092